Accepted Manuscript

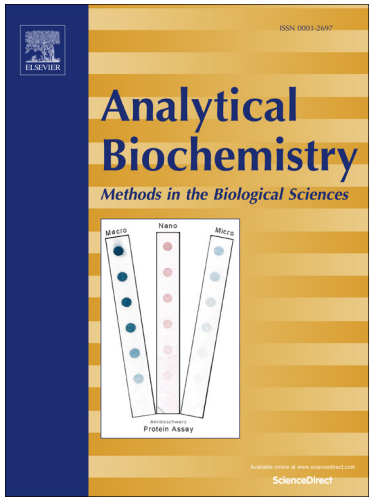

Evaluation of coumarin-based, fluorogenic P450 BM3 substrates and prospects for competitive inhibition screenings

Katharina Neufeld, Sonja Meyer zu Berstenhorst, Jörg Pietruszka

PII: S0003-2697(14)00121-3
DOI: http://dx.doi.org/10.1016/j.ab.2014.03.022
Reference: YABIO 11695

To appear in: *Analytical Biochemistry*

Received Date: 10 February 2014
Revised Date: 25 March 2014
Accepted Date: 28 March 2014

Please cite this article as: K. Neufeld, S. Meyer zu Berstenhorst, J. Pietruszka, Evaluation of coumarin-based, fluorogenic P450 BM3 substrates and prospects for competitive inhibition screenings, *Analytical Biochemistry* (2014), doi: http://dx.doi.org/10.1016/j.ab.2014.03.022

Title

Evaluation of coumarin-based, fluorogenic P450 BM3 substrates and prospects for competitive inhibition screenings[1]

Short title

Coumarin-based, fluorogenic P450 BM3 substrates

Authors

Katharina Neufeld*[a], Sonja Meyer zu Berstenhorst[a] and Jörg Pietruszka[a,b]

[a] Institut für Bioorganische Chemie der Heinrich-Heine-Universität Düsseldorf im Forschungszentrum Jülich, Stetternicher Forst, Geb. 15.8, 52426 Jülich (Deutschland).

E-Mail: j.pietruszka@fz-juelich.de; Fax: +49-2461-616196; Tel. +49-2461-614158.

[b] Institut für Bio- und Geowissenschaften (IBG-1: Biotechnologie), Forschungszentrum Jülich, Wilhelm-Johnen-Straße, 52425 Jülich (Deutschland).

Subject category for the table of contents

enzymatic assays and analyses

Abstract

Fluorescence-based assays for the cytochrome P450 BM3 monooxygenase from *Bacillus megaterium* address an attractive biotechnological challenge by facilitating enzyme engineering and the identification of potential substrates of this highly promising biocatalyst. In the present study, we used the scarcity of corresponding screening systems as an opportunity to evaluate a novel and continuous high-throughput assay for this unique enzyme. A set of nine catalytically-diverse P450 BM3 variants was constructed and tested toward the native-substrate-inspired fluorogenic substrate 12-(4-trifluoromethylcoumarin-7-yloxy)dodecanoic acid. Particularly high enzyme-mediated *O*-dealkylation yielding the fluorescent product 7-hydroxy-4-trifluoromethylcoumarin was observed with mutants containing the F87V substitution, with A74G/F87V showing the highest catalytic efficiency (0.458 min^{-1} μM^{-1}). To simplify the assay procedure and show its versatility, different modes of application were successfully demonstrated including i) the direct use of NADPH or its oxidized form $NADP^+$ along with diverse NADPH-recycling-systems for electron supply, ii) the use of cell-free lysates and whole-cell preparations as the biocatalyst source, and iii) its use for competitive inhibition screens to identify or characterize substrates and inhibitors. A detailed comparison with known, fluorescence-based P450 BM3 assays finally emphasizes the relevance of our contribution to the ongoing research.

Keywords: cytochrome P450 BM3, fluorescence-based assay, microtiter plate, high-throughput screening, P450 inhibition

Introduction

Cytochrome P450 monooxygenases (P450s)[2] form a diverse superfamily of heme-enzymes that are highly relevant for pharmaceutical, environmental and biocatalytic applications due to their ability to degrade toxic xenobiotics, metabolize drugs and catalyze the production of high-value fine chemicals [for selected reviews, see 1-7]. In this regard, the bacterial P450 BM3 monooxygenase from *Bacillus megaterium* (alias CYP102A1; EC 1.14.14.1) is one of the best studied and most widely used enzymes because of its advantageous properties plus the availability of large-scale production and purification protocols [8-10]. BM3 is a soluble and self-sufficient fusion protein, which was originally classified as a fatty acid hydroxylase [11]. Its published mutants are able to catalyze the oxygenation, mainly hydroxylation or epoxidation, of a variety of organic compounds in the presence of O_2 and NADPH with high efficiencies and unique selectivities, thereby illustrating the high potential and versatility of this biocatalyst [12,13]. Successful preparative scale applications further emphasize the superior catalytic features of this enzyme compared to other P450s [14-19]. Besides the production of fine chemicals, which is repeatedly mentioned as the major field of application for P450 BM3, this biocatalyst has attracted growing interest for the synthesis of human metabolites (for the approval of new therapeutics through toxicological characterization of metabolic profiles of potential drugs) and lead structure diversification in the last decade [20-24]. This interest can be ascribed to the high sequential, structural and functional similarities of the bacterial enzyme with eukaryotic counterparts and the high consensus among the product profiles of P450 BM3 mutants and mammalian P450s along with comparatively higher activity and stability as well as advantageous handling of the first-mentioned due to its bacterial origin [25-28]. In the past, identification of beneficial variants

possessing highly expanded substrate spectra and improved catalytic properties has been the result of successful protein engineering using predominantly colorimetric assays. The majority of these are indirect or end-point assays, so that the reaction rates are either inferred from the decrease or increase of a participating reagent or product formation is retrospectively ascertained upon a color-forming transformation [29]. The first direct and continuous assay for P450 BM3 was established by Schwaneberg *et al*. in 1999 and uses *p*-nitrophenol ethers as chromogenic substrates; *O*-dealkylation proceeds through P450 BM3-catalyzed ω-hydroxylation yielding an instable hemiacetal, which decomposes into an aldehyde and the spectrophotometrically detectable chromophore *p*-nitrophenolate [30]. Fluorescence-based assays are considered to be superior compared to their colorimetric alternatives due to higher sensitivity and lower susceptibility to interference by contaminants and assay components [31]. Thus, for assaying metagenomes or human P450s - both challenging applications due to low enzyme contents and activities – the state-of-the-art are ethers of fluorescent phenols such as resorufin or umbelliferone which follow the same mode of action [32-34]. Furthermore, fluorescence-based assays can be used for competitive inhibition screens, enabling the rapid identification of potential enzyme substrates or inhibitors, as these compounds compete with the fluorogenic substrate in the P450 reaction and thereby decelerate its output [35-38]. The first fluorescence-based assay for P450 BM3 using alkoxyresorufins as drug-like substrates was described by Lussenburg *et al*. in 2005 and extended to various resorufin derivatives [39-42]. Moreover, Kim *et al*. studied alkoxycoumarins as promising P450 BM3 substrates and Ruff *et al*. reported of 7-benzyloxy-3-carboxycoumarin ethyl ester (BCCE) as a surrogate substrate [43-44]. Despite the many benefits of fluorogenic substrates, the small number of known

compounds highlights the importance of developing new fluorescence-based screening systems for this biotechnologically important enzyme. This need is further encouraged by the practical advantages of corresponding inhibition assays over available alternatives for the structure- and product-independent identification of P450 BM3 substrates such as i) $NADP^+$/NADPH- or O_2-based detection systems, ii) the spectroscopic proof of substrate binding *via* detecting the low-to-high spin state transition of the heme iron, iii) the covalent labeling of P450 BM3 with a fluorophore functioning as a reporter for ligand screening, or iv) *in silico* approaches, all of which suffer from high costs, low sensitivity, are laborious, require purified enzymes and involve false positives or negatives [29,45-48].

In this study, we describe a continuous, fluorescence-based, high-throughput assay for detecting P450 BM3 hydroxylation activity by employing a set of catalytically-diverse P450 BM3 mutants and a novel, native-substrates-inspired, coumarin-based surrogate substrate. To estimate the performance of this compound in a wider sense, the assay was further simplified toward the application with diverse NADPH-recycling-systems plus whole-cell samples and applied to quantitative and qualitative competitive inhibition screenings. A comparison with existing assays highlights the relevance of the presented approach.

Materials and Methods

Reagents, enzymes and strains

All chemicals were purchased from standard suppliers and used without further purification except for petroleum ether (PE) and EtOAc, which were distilled prior to use. Preparative column chromatography was performed using silica gel 60 (particle size 0.040-0.063 mm, 230-240 mesh). NADP-Na_2 was kindly provided by Jülich Fine Chemicals. The P450 BM3-containing pET28a(+) plasmids were available as previously mentioned [49]; for construction of P450 BM3 variants see Sect. 5 in the Supporting Information. Enzymes for DNA manipulation and dNTPs were procured from Fermentas. *Pfu* DNA polymerase was a kind gift from Prof. K.-E. Jaeger (IMET, HHU Düsseldorf, Germany). GDH and ADH_{LK} were generously provided by Prof. W. Hummel (IMET, HHU Düsseldorf, Germany; glucose dehydrogenase, alcohol dehydrogenase from *Lactobacillus kefir*) and FDH (Jülich Fine Chemicals; formate dehydrogenase) was a gift from Prof. M. Pohl (IBG-1: Biotechnology, FZ Jülich, Germany); for determination of enzyme activities see Sect. 4 in the Supporting Information. Lysozyme from chicken egg white (#62971), CalB (*Candida antarctica* lipase B immobilized on acrylic resin, #L4777), RedTaq-Mix (#R2523), and oligonucleotides were purchased at Sigma-Aldrich. *E. coli* strains DH5α or BL21 (DE3) were used for DNA manipulations and heterologous protein expression, respectively.

Analytical methods

Analytical TLC was carried out on Polygram® SIL G/UC245 plastic sheets (Macherey Nagel). Aliphatic compounds were detected by oxidative staining (applying a mixture of 300 mL AcOH, 6 mL conc. H_2SO_4 and 3 mL *p*-anisaldehyde and color development with a hot-air blow dryer) and aromatic compounds were visualized by UV irra-

diation at 254 nm or observed with the naked eye. ^{1}H, ^{13}C and ^{19}F NMR spectra were recorded on an Advance/DRX 600 nuclear magnetic resonance spectrophotometer (Bruker) at rt and 600, 151 and 565 MHz, respectively. Chemical shifts (δ) are given in ppm relative to tetramethylsilane as an internal standard or relative to the solvent [^{1}H: δ($SiMe_4$) = 0.00 ppm, δ(DMSO) = 2.50 ppm, δ(pyridine) = 8.74 ppm; ^{13}C: δ($CDCl_3$) = 77.16 ppm, δ(DMSO) = 39.52 ppm]. Assignment was performed by means of H-COSY-, HSQC- and HMBC-experiments. IR measurements were conducted on a SpectrumOne spectrometer (PerkinElmer). Melting points were determined using a Melting Point B-450 instrument (Büchi). ESI-MS data were recorded using a MAT LC-Q mass spectrometer (Finnigan). Combustion analyses and HRMS measurements were carried out by the ZEA-3 of FZ Jülich.

Synthesis

7-Hydroxy-4-trifluoromethylcoumarin (**1**) was synthesized according to a known procedure [50]. Resorcinol (**2**) (440 mg, 4.00 mmol), ethyl 4,4,4- trifluoroacetoacetate (**3**) (736 mg, 585 µL, 4.00 mmol) and trifluoroacetic acid (2 mL) were heated in an oven-dried 10 mL heavy-walled microwave reaction vessel equipped with a cross-shaped, magnetic stirring bar and closed with a snap cap to 100 °C for 30 min in a Discovery microwave (CEM). After cooling to rt, the reaction mixture was slowly added to an ice:water-mixture (120 mL, 1:1) under vigorous stirring. The pink precipitate was filtered off, washed with cooled dest. water and dried under reduced pressure. Chromatography on silica gel with PE:EtOAc (8:2) provided the fluorescent dye **1** (497 mg, 2.16 mmol, 54%) as a colorless solid. The analytical data were generally consistent with those previously reported [50,51]. **TLC**: R_f 0.58 (PE:EtOAc, 1:1); **mp**: 182 °C; **IR** (ATR, film): 3395 (O-H), 3106, 1893, 1766, 1709 (C=O), 1630, 1607, 1575, 1519, 1494, 1441, 1405, 1362, 1337, 1284, 1214, 1190, 1158, 1120, 1008,

963, 891, 856, 821, 798, 750, 743, 721, 710, 670, 657 cm^{-1}; **^{1}H NMR** (DMSO-*d_6*): δ = 6.76 (s, 1 H, 3-H), 6.83 (d, *J* = 2.4 Hz, 1 H, 8-H), 6.91 (dd, *J* = 8.9, 2.4 Hz, 1 H, 6-H), 7.56 (dd, *J* = 8.9, 1.6 Hz, 1 H, 5-H), 10.95 (brs, 1 H, OH) ppm; **^{13}C NMR** (DMSO-*d_6*): δ = 103.2 (C-8), 105.3 (C-8a), 112.0 (q, J_{C-F} = 5.8 Hz, C-3), 114.1 (C-6), 121.8 (q, J_{C-F} = 275.8 Hz, C-4), 126.2 (C-5), 139.8 (q, J_{C-F} = 31.9 Hz, C-4a), 156.0 (CF_3), 158.9 (C-2), 162.2 (C-7) ppm; **^{19}F NMR** (DMSO-*d_6*): δ = -63.6 ppm; **HRMS** (ESI): calcd. for $[C_{10}H_6F_3O_3]^+$ ($[M+H]^+$): 231.02636; found: 231.02635; **Anal.**: calcd. for $C_{10}H_5F_3O_3$: C, 52.19; H, 2.19; found: C, 52.03 $\pm$ 0.09; H, 2.23 $\pm$ 0.03.

Methyl 12-bromododecanoate (**7**) was synthesized *via* a standard procedure by dissolving 12-bromododecanoic acid (**6**) (1.0 g, 3.59 mmol) in dry MeOH (10 mL) containing conc. H_2SO_4 (200 µL) under argon atmosphere and heating to reflux for 15 h. MeOH was removed under reduced pressure, the residual diluted with EtOAc (100 mL), washed with a saturated $NaHCO_3$-solution (3 x 20 mL) and brine (2 x 20 mL), dried with $MgSO_4$ and the solvent was removed under reduced pressure. Chromatography on silica gel with PE:EtOAc (97.5:2.5) provided the desired ester **7** (974 mg, 3.32 mmol, 93%) as colorless oil. The analytical data were generally consistent with those previously reported [52-54]. **TLC**: R_f 0.45 (PE:EtOAc, 9:1); **IR** (ATR, film): 2926, 2854, 1740 (C=O), 1459, 1436, 1362, 1252, 1242, 1197, 1171, 1120, 1103, 1012, 881, 723 cm^{-1}; **^{1}H NMR** ($CDCl_3$): δ = 1.23-1.35 (m, 12 H, 4-H to 9-H), 1.42 (tt, *J* = 7.4, 7.2 Hz, 2 H, 10-H), 1.62 (tt, *J* = 7.6, 7.4 Hz, 2 H, 3-H), 1.85 (tt, *J* = 7.4, 6.9 Hz, 2 H, 11-H), 2.30 (t, *J* = 7.6 Hz, 2 H, 2-H), 3.41 (t, *J* = 6.9 Hz, 2 H, 12-H), 3.67 (s, 3 H, OCH_3) ppm; **^{13}C NMR** ($CDCl_3$): δ = 25.1 (C-3), 28.3 (C-10), 28.9, 29.3, 29.4, 29.5, 29.5, 29.6 (C-4 to C-9), 33.0 (C-11), 34.2 (C-12), 34.3 (C-2), 51.6 (OCH_3), 174.5 (C-1) ppm; **HRMS** (ESI): calcd. for $[C_{13}H_{26}O_2{}^{79}Br/{}^{81}Br]^+$ ($[M+H]^+$): 293.11107/ 295.10902; found: 293.11113/ 295.10908.

Methyl 12-(4-trifluoromethylcoumarin-7-yloxy)dodecanoate (**5**) was synthesized according to a known procedure [55]. Dye **1** (549 mg, 2.39 mmol) and anhydrous K_2CO_3 (363 mg, 2.63 mmol) were incubated in DMF (10 mL) under argon atmosphere for 2 h at rt. Subsequently, bromide **7** (700 mg, 2.39 mmol) was added and the reaction was heated to 90 °C for 15 h. After cooling to rt, the reaction mixture was diluted with EtOAc (100 mL), washed with saturated $NaHCO_3$-solution (2 x 30 mL) and brine (2 x 30 mL), dried with $MgSO_4$ and the solvent was removed under reduced pressure. Chromatography on silica gel with PE:EtOAc (95:5) provided the fluorogenic substrate **5** (1.01 g, 2.28 mmol, 95%) as a colorless solid. **TLC**: R_f 0.76 (PE:EtOAc, 7:3); **mp**: 85 °C; **IR** (ATR, film): 3096, 2932, 2918, 2853, 1736 (C=O), 1722 (C=O), 1611, 1562, 1517, 1473, 1440, 1427, 1418, 1408, 1395, 1378, 1348, 1330, 1278, 1270, 1209, 1193, 1160, 1129, 1080, 1070, 1057, 1025, 1008, 982, 970, 958, 940, 884, 871, 847, 835, 827, 802, 752, 742, 722, 710, 668 cm^{-1}; **^{1}H NMR** ($CDCl_3$): δ = 1.24-1.40 (m, 12 H, 4-H to 9-H), 1.47 (m_c, 2 H, 10-H), 1.62 (m_c, 2 H, 3-H), 1.82 (m_c, 2 H, 11-H), 2.30 (t, J = 7.6 Hz, 2 H, 2-H), 3.67 (s, 3 H, CH_3), 4.04 (t, J = 6.5 Hz, 2 H, 12-H), 6.60 (s, 1 H, 3-H_{Ar}), 6.86 (d, J = 2.5 Hz, 1 H, 8-H_{Ar}), 6.91 (dd, J = 9.0, 2.5 Hz, 1 H, 6-H_{Ar}), 7.61 (dd, J = 9.0, 1.7 Hz, 1 H, 5-H_{Ar}) ppm; **^{13}C NMR** ($CDCl_3$): δ = 25.1 (C-3), 26.0 (C-10), 29.0 (C-11), 29.6, 29.6, 29.5, 29.4, 29.4, 29.3 (C-4 to C-9), 34.2 (C-2), 51.6 (CH_3), 69.0 (C-12), 102.0 (C_{Ar}-8), 106.9 (C-8a), 112.1 (q, J_{C-F} = 5.8 Hz, C_{Ar}-3), 113.9 (C_{Ar}-6), 121.7 (q, J_{C-F} = 276.3 Hz, C_{Ar}-4), 126.4 (C_{Ar}-5), 141.7 (q, J_{C-F} = 32.7 Hz, C-4a), 156.5 (CF_3), 159.6 (C_{Ar}-2), 163.3 (C_{Ar}-7), 174.4 (C-1) ppm; **^{19}F NMR** ($CDCl_3$): δ = -64.7 ppm; **HRMS** (ESI): calcd for $[C_{23}H_{30}F_3O_5]^+$ ($[M+H]^+$): 443.20399; found: 443.20399; **Anal.**: calcd. for $C_{23}H_{29}F_3O_5$: C, 62.43; H, 6.61; found: C, 62.49 ± 0.06; H, 6.63 ± 0.02.

12-(4-Trifluoromethylcoumarin-7-yloxy)dodecanoic acid (**4**) was synthesized *via* a standard procedure by dissolving ester **5** (364 mg, 0.82 mmol) in THF (10 mL). KOH (346 mg, 6.17 mmol) dissolved in 10 mL H_2O was slowly added at 0 °C, the reaction was incubated for 2 h on ice and subsequently warmed to rt. Full conversion was confirmed by TLC after additional 5 h. The reaction mixture was diluted with ice-cold 1 M aqueous HCl (40 mL) and extracted with CH_2Cl_2 (4 x 30 mL). The combined organic phases were dried with $MgSO_4$ and the solvent was removed under reduced pressure. Chromatography on silica gel with PE:EtOAc (7:3) provided the desired acid **4** (350 mg, 0.82 mmol, quant.) as a colorless solid. **TLC**: R_f 0.43 (PE:EtOAc, 7:3); **mp**: 90 °C; **IR** (ATR, film): 3085, 2921, 2852, 1757, 1733 (C=O), 1698 (C=O), 1611, 1557, 1517, 1474, 1432, 1412, 1402, 1364, 1348, 1325, 1305, 1296, 1276, 1244, 1213, 1189, 1168, 1138, 1117, 1084, 1039, 1029, 1017, 1002, 984, 976, 958, 942, 868, 857, 833, 799, 785, 752, 735, 719, 711, 685 cm^{-1}; **^{1}H NMR** ($CDCl_3$): δ = 1.24-1.40 (m, 12 H, 4-H to 9-H), 1.47 (m_c, 2 H, 10-H), 1.63 (m_c, 2 H, 3-H), 1.82 (m_c, 2 H, 11-H), 2.35 (t, *J* = 7.5 Hz, 2 H, 2-H), 4.04 (t, *J* = 6.5 Hz, 2 H, 12-H), 6.61 (s, 1 H, 3-H_{Ar}), 6.86 (d, *J* = 2.5 Hz, 1 H, 8-H_{Ar}), 6.91 (dd, *J* = 9.0, 2.5 Hz, 1 H, 6-H_{Ar}), 7.61 (dd, *J* = 9.0, 1.7 Hz, 1 H, 5-H_{Ar}) ppm; **^{13}C NMR** ($CDCl_3$): δ = 24.8 (C-3), 26.0 (C-10), 29.0 (C-11), 29.6, 29.6, 29.5, 29.4, 29.3, 29.2 (C-4 to C-9), 34.1 (C-2), 69.0 (C-12), 102.0 (C_{Ar}-8), 107.0 (C-8a), 112.2 (q, J_{C-F} = 5.8 Hz, C_{Ar}-3), 113.9 (C_{Ar}-6), 121.7 (q, J_{C-F} = 276.0 Hz, C_{Ar}-4), 126.4 (C_{Ar}-5), 141.8 (q, J_{C-F} = 32.9 Hz, C-4a), 156.5 (CF_3), 159.6 (C_{Ar}-2), 163.3 (C_{Ar}-7), 174.8 (C-1) ppm; **^{19}F NMR** ($CDCl_3$): δ = -64.7 ppm; **MS** (ESI): *m/z* (%) = 429 [$(M+H)^+$]; **Anal.**: calcd. for $C_{22}H_{27}F_3O_5$: C, 61.67; H, 6.35; found: C, 61.87 ± 0.05; H, 6.42 ± 0.01.

Methyl 12-(3H-phenoxazin-3-one-7-yloxy)dodecanoate (**19**) was prepared as described for ester **5** except that higher solvent amounts and longer reaction time were

needed due to lower solubility. The reaction mixture containing resorufin (**18**) (369 mg, 1.73 mmol), anhydrous K_2CO_3 (264 mg, 1.90 mmol) and bromide **7** (507 mg, 1.73 mmol) in DMF (24 mL) was heated for 2 d. The dilution ensued with 2 L EtOAc and each wash step was performed with 500 mL. Chromatography on silica gel with PE:EtOAc (7:3→EtOAc) provided the fluorogenic substrate **19** (452 mg, 1.06 mmol, 61%) as an orange solid. **TLC**: R_f 0.64 (PE:EtOAc, 1:1); **mp**: 128 °C; **IR** (ATR, film): 3083, 3053, 2995, 2920, 2850, 1730 (C=O), 1644, 1604, 1589, 1564, 1505, 1483, 1472, 1448, 1428, 1415, 1394, 1369, 1339, 1317, 1271, 1233, 1213, 1203, 1183, 1169, 1159, 1120, 1102, 1036, 1024, 1011, 995, 979, 958, 924, 905, 888, 862, 836, 818, 780, 766, 746, 734, 721, 711 cm^{-1}; **^{1}H NMR** ($CDCl_3$): δ = 1.24-1.40 (m, 4-H to 9-H, 12 H), 1.47 (tt, *J* = 7.3, 7.3 Hz, 2 H, 10-H), 1.62 (tt, *J* = 7.6, 7.6 Hz, 2 H, 3-H), 1.84 (tt, *J* = 7.3, 6.5 Hz, 2 H, 11-H), 2.30 (t, *J* = 7.5 Hz, 2 H, 2-H), 3.67 (s, 3 H, CH_3), 4.06 (t, *J* = 6.5 Hz, 2 H, 12-H), 6.32 (d, *J* = 2.6 Hz, 1 H, 8-H_{Ar}), 6.80 (d, *J* = 2.0 Hz, 1 H, 10-H_{Ar}), 6.83 (dd, *J* = 9.8, 2.0 Hz, 1 H, 2-H_{Ar}), 6.93 (dd, *J* = 8.9, 2.6 Hz, 1 H, 6-H_{Ar}), 7.42 (d, *J* = 9.8 Hz, 1 H, 3-H_{Ar}), 7.70 (d, *J* = 8.9 Hz, 1 H, 5-H_{Ar}) ppm; **^{13}C NMR** ($CDCl_3$): δ = 25.1 (C-3), 26.1 (C-10), 29.1 (C-11), 29.6, 29.6, 29.5, 29.4, 29.4, 29.3 (C-4 to C9), 34.3 (C-2), 51.6 (CH_3), 69.3 (C-12), 100.6 (C_{Ar}-10), 106.8 (C_{Ar}-8), 114.3 (C_{Ar}-6), 128.4 (C-4a), 131.7 (C_{Ar}-5), 134.3 (C_{Ar}-2), 134.8 (C_{Ar}-3), 145.5 (C-8a), 145.9 (C-3a), 150.0 (C-9a), 163.5 (C_{Ar}-7), 174.5 (C-1), 186.4 (C_{Ar}-1) ppm; **HRMS** (ESI): calcd. for $[C_{25}H_{32}NO_5]^+$ ($[M+H]^+$): 426.22750; found: 426.22736; **Anal.**: calcd. for $C_{25}H_{31}NO_5$: C, 70.57; H, 7.34; N, 3.29; found: C, 70.40 ± 0.04; H, 7.32 ± 0.02; N, 3.26 ± 0.02.

12-(3H-Phenoxazin-3-one-7-yloxy)dodecanoic acid (**20**) was synthesized according to a known procedure [30]. Ester **19** (156 mg, 0.37 mmol) was dissolved in 500 mL acetone/buffer (100 mM KPi-buffer, pH 8.0, 80% acetone), CalB (2 kU) was added

and the reaction was incubated for 2 d at 37 °C and 140 rpm under exclusion of light. The catalyst was removed by filtration, acetone was evaporated under reduced pressure, 1 M aqueous HCl was added to adjust a pH of 1-2 and the precipitated product was filtered off. Washing with cooled dest. water and drying under reduced pressure gave the desired acid **20** (133 mg, 0.32 mmol, 88%) as an orange solid. **TLC**: R_f 0.33 (PE:EtOAc, 1:1); **mp**: 200 °C; **IR** (ATR, film): 3079, 2939, 2916, 2850, 1717 (C=O), 1646, 1607, 1577, 1554, 1504, 1487, 1470, 1435, 1409, 1367, 1341, 1331, 1289, 1267, 1233, 1215, 1202, 1175, 1164, 1123, 1110, 1085, 1068, 1054, 1019, 988, 973, 935, 911, 889, 862, 849, 837, 793, 762, 730, 716, 654 cm^{-1}; **^{1}H NMR** (pyridine-d_5): δ = 1.19-1.36 (m, 5-H to 9-H, 10 H), 1.37-1.51 (m, 4 H, 4-H, 10-H), 1.73-1.87 (m, 4 H, 3-H, 11-H), 2.55 (t, J = 7.3 Hz, 2 H, 2-H), 4.10 (t, J = 6.4 Hz, 2 H, 12-H), 6.48 (d, J = 1.7 Hz, 1 H, H_{Ar}), 6.97 (dd, J = 9.8, 1.7 Hz, 1 H, H_{Ar}), 7.01 (s, 1 H, H_{Ar}), 7.11 (d, J = 8.8 Hz, 1 H, H_{Ar}), 7.51 (d, J = 9.8 Hz, 1 H, H_{Ar}), 7.85 (d, J = 8.8 Hz, 1 H, H_{Ar}) ppm; **HRMS** (ESI): calcd. for $[C_{24}H_{30}NO_5]^+$ ($[M+H]^+$): 412.21185; found: 412.21185; **Anal.**: calcd. for $C_{24}H_{29}NO_5$: C, 70.05; H, 7.10; N, 3.40; found: C, 69.72 ± 0.14; H, 7.10 ± 0.04; N, 3.40 ± 0.01.

Absorption and fluorescence measurements in MTPs

Absorption and fluorescence measurements were carried out under aerobic conditions using an Infinite® M1000 spectrophotometer plate reader (Tecan) equipped with the i-control™ software in colorless, flat-bottomed 96-well and black, flat-bottomed 384-well microtiter plates (MTPs; Grainer Bio-One) at 30 °C applying a final volume of 200 and 100 µL/well, respectively. The excitation and emission wavelengths used were $\lambda_{ex:}$ 420 nm/ $\lambda_{em:}$ 500 nm for **1** and $\lambda_{ex:}$ 530 nm/ λ_{em}: 595 nm for **18** (bandwidth 5 nm). All experiments were performed in a KPi/Tris-buffer-mixture (BM3 buffer, pH 7.8, 50 mM KPi, 50 mM Tris/HCl). Stock solutions and dilutions of sub-

strates, fluorophores and inhibitors were prepared in DMSO (heating to 80 °C facilitated compound solution). Fluorescence intensities were converted to product concentrations using calibration curves measured for each experiment individually by addition of **1** or **18** (serial 2:3 dilutions plus blank values, max. final concentration (f. c.) 10 µM) instead of substrate to the assay mixtures. All measurements were performed in triplicate.

*Determination of substrate **4** O-dealkylation:* Protein expression in deep-well plates and preparation of cell-free crude lysates (CCLs) for assaying *O*-dealkylation activities of the constructed P450 BM3 variants toward substrate **4** were performed as previously described [49]. Reactions composed of 70 µL BM3 buffer, 10 µL CCL and 10 µL substrate **4** (100 µM) were initialized by addition of 10 µL NADPH (3 mM in H_2O). Formation of **1** was monitored for 5 min and evaluation of data was conducted in end-point mode by subtracting the initial fluorescence intensity from those obtained after a 5-min reaction and normalizing the values according to the empty vector negative control.

To examine whether NADPH-recycling-systems are likewise suitable to support P450 BM3-mediated *O*-dealkylation, the same conditions were used and 10 µL of $NADP^+$-coenzyme-cosubstrate-mixtures were added to initialize the reactions: GDH-samples contained 5 µL glucose (200 mM in H_2O) and 12.8 mU GDH, FDH-samples 5 µL sodium formate (2 M in H_2O) and 3.3 mU FDH and ADH-samples 5 µL isopropanol (200 mM in H_2O supplemented with 20 mM $MgCl_2$) and 88 mU ADH, respectively, along with 0.2 µL $NADP^+$ (50 mM in H_2O) in BM3 buffer (add to 10 µL).

To examine whether CCLs can be substituted with *E. coli* whole-cells plus lysozyme or polymyxin B treated samples, the previous experiment was repeated using the

GDH-recycling-system. Intact whole-cell samples were prepared by resuspending the cell pellets in 240 µL 50 mM KPi buffer (pH 7.5). Lysozyme-treated samples were obtained in the same manner except that the buffer contained 5 mg mL^{-1} lysozyme and the samples were incubated at 37 °C and 900 rpm for 1 h before use. Polymyxin B-treated samples were generated from whole-cell samples by addition of 10 µL polymyxin B (0.75 mM in buffer) to 10 µL cell suspension and 60 µL BM3 buffer plus incubation for 15 min. NADPH-supply was a prerequisite to observe activity in all cases.

Determination of kinetic parameters: Flask expressions, protein purification and quantification of P450 BM3 contents were performed as previously described [49]. Based on pre-test results, samples for kinetic measurements were composed of 5.3 pmol GV, 15.8 pmol F87V, 29.2 pmol GQ and 17.0 pmol F87A for substrate **4**, 53.0 pmol GV and 31.6 pmol F87V for substrate **5** and 117.8 pmol GQ for substrate **19** in 80 µL BM3 buffer, respectively (see Fig. S5 in the Supporting Information). Hereto, 10 µL of substrate (serial 2:3 dilutions plus blank values; max. f. c. for **4** was 133 µM, for **5** 70 µM and for **19** 9.7 µM, respectively) were added and the mixtures were pre-incubated for 5 min at 900 rpm and rt before reactions were initialized by addition of 10 µL ADH-recycling-system. Formation of **1** was monitored for 2-10 min. Reaction rates were calculated based on the linear portions of curves and plotted against the substrate concentrations. Using the non-linear regression tool of OriginPro 9.0G, data showing sigmoidal kinetics were fitted using the Hill equation and data indicating excess-substrate inhibition were fitted using a modified Hill equation: $y = v_{max} \bullet x/(x^2/K_i + K_M + x)$ [56].

Qualitative inhibition screening: The ability of the established assay to identify ligands of P450 BM3 was tested with known non-substrates (caffeine **16** and iso-octane **17**), substrates (myristic acid **10**, naphthalene **11** and methyl 3-methoxy-2-methylbenzoate **12**) and inhibitors (ketoconazole **13**, imidazole **14** and cyanide **15**). Flask expression and preparation of CCLs was performed as described elsewhere except that the BM3 buffer was used [49]. Samples containing 27.6 pmol GV or 48.4 pmol F87V in 80 µL BM3 buffer, 5 µL substrate **4** (200 µM) and 5 µL compound of interest (test samples with varying concentrations: 100, 20 and 2 mM for **16**, **17**, **11**, **12** and **14**; 4, 2 and 0.4 µM for **10**; 100, 20 and 4 µM for **13** and 100, 20, 2 and 0.4 µM for **15**) or 5 µL DMSO (reference samples) were pre-incubated for 5 min at 900 rpm and rt before reactions were initialized by addition of 10 µL GDH-recycling-system. Formation of **1** was monitored for 5 min and evaluation was conducted in end-point mode as described above. The results were normalized relative to the activity obtained in absence of a probe compound and a threshold value of 90% was defined upon which enzyme inhibition was stated.

Quantitative inhibition screening: The ability of the established assay to provide IC_{50} values was tested with the known non-native substrate **12** and purified P450 BM3 F87A. Samples containing 54.7 pmol F87A in 80 µL BM3 buffer, 5 µL substrate **4** (300 µM) and 5 µL compound **12** (test samples: serial 2:3 dilution; max. f. c. 1 M) or 5 µL DMSO (reference sample) were pre-incubated for 5 min at 900 rpm and rt before reactions were initialized by addition of 10 µL ADH-recycling-system. Formation of **1** was monitored for 10 min and evaluation was conducted in end-point mode as described above. The obtained inhibition values were plotted against the concentration of **12** and data were fitted using the Michaelis-Menten equation.

Results and Discussion

Assay-related fluorophore selection and synthesis

Coumarin derivatives have proven to be excellent fluorescence markers and are nowadays routinely applied for the generation of diverse surrogate substrates [57,58]. In the present approach, 7-hydroxy-4-trifluoromethylcoumarin (**1**) (HTC) was favored due to its advantageous features related to P450 catalysis. In contrast to other commonly used fluorophores, HTC **1** ensures lower background signals and higher signal intensities as its excitation and emission spectra are shifted to higher wavelengths. Thus, the overlap with the optical characteristics of assay components is minimized and interference with NADPH can be eliminated [59]. Furthermore, the comparatively low pK_a value of 6.8 enables screening at slightly basic pH, which is beneficial as P450 BM3 shows its highest activity around pH 7 [60]. In the present study, λ_{ex}/ λ_{em} were set to 420/ 500 nm and a pH of 7.8 was selected as a compromise between enzyme activity and assay sensitivity (for a detailed illustration of the advantageous features of HTC **1**, see Sect. 1 in the Supporting Information). Moreover, while studying the P450 BM3-catalyzed oxygenation of 7-ethoxycoumarin, Kim *et al*. found most of the highly active P450 BM3 mutants to favor the 3-hydroxylation over the *O*-deethylation reaction [43]. We assumed that the trifluoromethyl moiety in **1** could shift the enzyme's preference toward *O*-dealkylation through steric effects, thereby not providing a P450 BM3 target since C-F bonds are considered to be inert [61-64]. Compound **1** was initially provided *via* a Pechmann reaction from resorcinol (**2**) and ethyl 4,4,4-trifluoroacetoacetate (**3**) according to a procedure of Katkevičs *et al.* in 54% yield (Scheme 1) [50]. However, due to ongoing efforts in assay research, this dye has recently become commercially affordable.

Synthesis of novel, fluorogenic BM3 substrates

Referring to the idea of Schwaneberg *et al.* for the *p*-nitrophenol-based, colorimetric P450 BM3 assay, in the present approach a fluorogenic P450 BM3 substrate bearing structural similarity to the native fatty acid substrates was envisaged [30]. Dodecanoic acid was selected as the substrate synthon and the HTC-labeled compound methyl 12-(4-trifluoromethylcoumarin-7-yloxy)dodecanoate (**4**) could be obtained from 12-bromododecanoic acid (**6**) and fluorophore **1** in an overall yield of 88% in three steps (Scheme 2). Bromide **6** was first protected to the corresponding methyl ester **7** in 93% yield, which was subsequently applied for the alkylation of **1** to give ester **5** in 95% yield; saponification under basic conditions provided the desired acid **4** quantitatively. Subsequently, the optical properties of substrates **4** and **5** and their solubility under assay conditions were investigated. Fig. 1 illustrates a shift of the absorption, excitation and emission spectra of these compounds to lower wavelengths compared to those of **1**, the optimal wavelengths being $\lambda_{abs}/\lambda_{ex}$: 335 nm and λ_{em}: 425 nm for **4**, λ_{abs}: 340 nm, λ_{ex}: 330 nm, and λ_{em}: 410 nm for **5** plus λ_{abs}: 390 nm, λ_{ex}: 380 nm, and λ_{em}: 500 nm for **1**. This shift ensures selective excitation and detection of HTC **1** in the presence of substrates **4** and **5** and proves the latter to be suitable fluorogenic substrates. Further, the ethers exhibit minor fluorescence intensities compared to HTC **1** by a factor of 6 and 11 for **4** and **5**, respectively ($\lambda_{ex}/\lambda_{em}$: **1**: 4164 a.u.; **4**: 698 a.u.; **5**: 371 a.u.), which is consistent with the 'blocked' character of **1** within these compounds. Solubility was examined by preparing serial dilutions of ethers, addition of buffer and measuring absorption at 600 nm to verify precipitation. Limits were determined to be 197 µM for ether **4** and 74 µM for ether **5**, respectively (see Sect. 2 in the Supporting Information).

Construction of the enzyme library

A small enzyme library consisting of nine P450 BM3 mutants was constructed to provide a versatile catalyst pool for the evaluation of the planned fluorescence-based assay. Literature-known mutants noted for wide substrate spectra, distinguishable product profiles and the ability to oxygenate sterically demanding compounds were assumed to be particularly suitable regarding surrogate substrate **4** and thus, seven of the selected variants contained the A74G (G), F87V (V) or L188Q (Q) substitution and combinations thereof. Especially the F87V single and the GVQ triple mutant have been repeatedly examined in the context of non-natural substrates in general and sterically demanding compounds in particular [65-74]. The F87A variant was also chosen due to its unique catalytic efficiency, which gave rise to iterated and extensive studies, and the WT enzyme was included for the sake of completeness [75-77]. Generation of the different variants was achieved by site-saturation mutagenesis.

Determination of P450 BM3-mediated *O*-dealkylation

The generally accepted principle of the metabolism of fluorogenic ether substrates into their highly fluorescent phenols by P450s is provided in Scheme 3 using the example of substrate **4**. *O*-dealkylation proceeds *via* enzyme-catalyzed ω-hydroxylation yielding the instable hemiacetal **8** as intermediate, which releases fluorophore **1** and aldehyde **9** upon spontaneous decomposition [30]. For testing of generated P450 BM3 mutants regarding this reaction, enzyme expression was performed in 96-deep-well plates to simulate screening conditions. Cell-free crude lysates were obtained upon cell lysis using lysozyme and incubated in 384-well format with 10 µM of **4** in the presence of NADPH. To our delight, formation of HTC **1** was observed and the values shown in Fig. 2 indicate that particularly P450 BM3 variants con-

taining the F87V substitution exhibit high *O*-dealkylation ability. The highest value of 58.2 ± 4.3 pmol/5min was obtained for the double mutant GV and other P450 BM3 variants metabolized **4** only at low rates, which were clearly distinguishable from the empty vector background. These results confirm the crucial role of the F87V mutation in controlling the substrate specificity of P450 BM3 and prove the designed and synthezised compound **4** to be a suitable fluorogenic substrate for this monooxygenase.

Establishment of simplified assay procedures

Regarding high-throughput applications direct utilization of NADPH as the electron source is undesirable due to its high costs and low stability [78]. Use of $NADP^+$ along with an appropriate NADPH-recycling-system offers a solution to this problem and high versatility of the established assay was shown by successful application of different enzyme-coupled recycling-systems. A GDH/glucose-, a FDH/formate- and an ADH/isopropanol-system were selected as these are the most commonly used NADPH-recycling-systems for P450 catalysis [79]. In all cases the co-enzyme catalyzes the oxidation of the co-substrate (glucose, formate or isopropanol) and simultaneous reduction of $NADP^+$ to NADPH, providing the latter for the P450 BM3-mediated *O*-dealkylation. Initial tests were performed to determine appropriate co-enzyme and co-substrate concentrations, thereby ensuring the P450 BM3-catalyzed reaction to be the rate-determining step within the assay (data not shown). Subsequent screening of the P450 BM3 library using these NADPH-recycling-mixtures reproduced the previously observed activity pattern with the GV mutant giving the highest activity in all measurement series, even though the total values varied depending on the applied recycling-system (Table 1, upper part). To facilitate comparability, reaction rates were standardized to the GV results and the previous

experiment was included for comparison (Table 1, lower part). Observed differences between the different measurement series result from the nature of the NADPH-providing step and the P450 BM3 activity under the respective conditions. The GDH and FDH reactions are assumed to be irreversible as glucose is converted to gluconolactone, which decomposes to gluconic acid under assay conditions, and formate is converted to CO_2, which can depart from the reaction mixture. In both cases the pH of the assay solution is affected by formation of the co-product (decreasing and increasing effect in case of GDH and FDH, respectively), which has a major influence on the protonation state of HTC **1** and therefore, on the intensity of the fluorescence signal. Thus, besides the ability of the P450 BM3 variants to mediate *O*-dealkylation, their ratio of decoupling significantly contributes to the final screening results (decoupling denotes the amount of consumed NADPH not used for substrate oxidation). The ADH reaction reversibly yields acetone as the oxidized co-product. In contrast to the previous systems an impact on the pH can be excluded, but ADH-catalyzed oxidations of assay components are possible and a negative influence of acetone or isopropanol on the solvent-sensitive P450 BM3 enzyme is conceivable in common with a positive effect on substrate solubility in the presence of these co-solvents [80]. Based on these considerations, the higher values obtained with GDH- and ADH-recycling compared to those for the NADPH approach can be lead back to higher cofactor amount under the first mentioned conditions. In this, the comparatively minor values using GDH-recycling arise from acidification of the sample mixtures in the course of the reactions. Further, GDH- and ADH-promoted reactions revealed better reproducibility across replicates compared to the NADPH approach. On the contrary, the low values obtained with FDH-recycling indicate minor P450 BM3 activity in the presence of formate. To the best of our knowledge, this is the first

time a direct comparison between different NADPH-recycling-systems with respect to P450 BM3 activity is provided and all systems tested are superior over the G6PDH-recycling, which requires expensive glucose-6-phosphate as co-substrate and was exclusively applied in previous P450 BM3 fluorescence-based assays (G6PDH: glucose-6-phosphate dehydrogenase) [39,41,43].

To investigate whether the assay procedure can be further simplified by using turbid lysozyme-lysed, polymyxin B-permeabilized (polymyxin B is a pore-forming membrane protein) or untreated whole-cells as biocatalyst sources instead of laboriously generated lysates, three additional measurement series were conducted [81]. Screening was performed using GDH-recycling and the obtained values are presented in Table 2; the previously obtained cell-free crude lysate results were included for comparison. Lysozyme-lysed cells gave the highest consensus regarding the previous results, demonstrating that partition of insoluble cell components has only a negligible benefit. Whole-cell samples revealed approximately 7-fold lower product formation rates attributable to lower substrate accessibility to the enzyme as diffusion or active transport of substrate through *E. coli* membranes is required. Nevertheless, the expected activity pattern was fully reproduced, showing these samples to be likewise suited for the fluorescence-based assay. Interestingly, polymyxin B - although its benefit was emphasized by Schwaneberg *et al*. in the course of the *p*-nitrophenol-based P450 BM3 assay - had a negative effect by causing high background signals compared to untreated whole-cells in the present assay [82].

Characterization of kinetic parameters

Kinetic parameters are important measures for the interaction of substrates with their metabolizing enzymes. For characterization of surrogate substrate **4** and its ester

derivative **5**, three different P450 BM3 variants were expressed, purified and used for kinetic measurements. GV, F87V and GQ were chosen because they showed high, medium and low *O*-dealkylation activities in the previous experiments. Enzyme concentrations ensuring linearity between enzyme amount and *O*-dealkylation activity were determined in pre-tests for every enzyme-substrate-pair and the GQ-substrate **5**-pair was excluded from further investigations due to inappreciable activities. Enzyme kinetics were analyzed by measuring initial product formation rates in the presence of varied substrate amounts - the maximal value set according to previously determined solubility limits - using ADH-recycling (ensures pH stability). Results for GV with substrate **4** and F87V with substrate **5** are representatively shown in Fig. 3 and indicate inhibition of enzyme activity at high substrate concentrations (for a full overview, see Fig. S6 and Table S1 in the Supporting Information). The phenomenon of excess-substrate inhibition of P450s has repeatedly been discussed in the literature and has mainly been explained through simultaneous binding of two substrate molecules to the enzyme blocking its activity [83,84]. However, within the previous publications on fluorogenic P450 BM3 substrates, this behavior was neither observed for 7-ethoxycoumarin or BCCE nor for resorufin ethers [39-44]. Correlation of the obtained data considering excess-substrate inhibition gave the kinetic parameters K_M, v_{max}, K_i and n as listed in Table 3. The best catalytic efficiency was 0.458 min^{-1} μM^{-1} for the GV mutant with substrate **4** and represents one of the highest values ever observed for the P450 BM3-mediated *O*-dealkylation of fluorogenic ethers [39-44]. In addition, the catalytic efficiencies for acid **4** exceeded those for ester **5** by up to two orders of magnitude (even though the K_M values for the first were considerably higher), which is attributable to the higher native-substrate-resemblance of substrate **4** over **5**. The results further indicate a positive effect of the F87V

substitution on the P450 BM3 activity regarding both examined compounds, whereas the A74G mutation seems to enhance enzyme activity exclusively for substrate **4**. Moreover, the high Hill coefficients obtained for acid **4** (n = 1.7 - 2.2) suggest positive homotropic cooperativity, which is in accordance with the dimeric nature of the P450 BM3 enzyme, whereas cooperativity is significantly less distinct in case of ester **5** (n = 1.4) [85].

Establishment of a competitive inhibition screening

The preceding survey provided enzyme-substrate-pairs for competitive inhibition studies of P450 BM3 and the GV-substrate **4**-pair was selected to validate the assay's ability for detecting inhibition caused by known P450 BM3 substrates, non-substrates, and inhibitors. In detail, myristic acid (**10**) was selected as a native substrate, naphthalene (**11**) and methyl 2-methoxy-3-methylbenzoate (**12**) representted non-native substrates, ketoconazole (**13**), imidazole (**14**), and potassium cyanide (**15**) were tested as inhibitors, and caffeine (**16**) plus isooctane (**17**) served as non-substrates, as the latter are neither oxidized by P450 BM3 nor inhibit the enzyme [39,49,86-89]. Fluorescence interference or quenching attributable to these probe compounds was excluded *a priori* (data not shown). Moreover, K_M values serve as a guide for setting fluorogenic substrate concentrations for inhibition assays, because high sensitivity toward inhibition along with high signal intensity is assured at this concentration [59]. 10 µM of substrate **4** were used in the present study according to the obtained K_M of 12.4 ± 2.5 µM. The inhibitory effect of probe compounds on the *O*-dealkylation activity of GV toward **4** was quantified using varying probe compound concentrations depending on respective inhibition capacities, the latter mirroring the compounds' affinities to the enzyme. The obtained results are listed in Table 4 and attest to the inhibitory effect of all tested substrates

and inhibitors, whereas no significant influence on the reaction output was observed for non-substrates. The presence of 1 µM of the highly potent inhibitor ketoconazole (**13**) lowered the reaction outcome to 65 ± 4% and at 5 µM the enzyme's activity was almost completely inhibited, whereas in case of the non-native substrate **12** concentrations ≥1 mM needed to be applied for categorical results. Nevertheless, preparative biotransformation of **12** was shown in a previous study (K_M: 1.8 ± 0.2 mM for P450 BM3 mutant F87A/L188C, 0.6 mmol scale, 98% conversion, 73% yield [49]) and hence, the obtained results advise to use mM concentrations of non-natural substrates in P450 BM3 inhibition assays as successful preparative transformations of respective hits are likely, even though distinctly lower substance amounts are common [39,41]. Furthermore, the F87V mutant was subjected to the same experiment and the previously observed inhibition pattern was confirmed in the broadest sense (Table 4). However, a closer look reveals varieties between the different P450 BM3 catalysts, as the extent of F87V inhibition was lower in case of imidazole (**14**) and substrate **12** when compared to the GV results, whereas upon addition of myristic acid (**10**) and naphthalene (**11**) higher inhibition was observed. These differences are probably attributable to the different K_M values of both P450 BM3 mutants for the compounds tested and conversion studies indeed showed GV to be the better catalyst regarding substrate **12** (data not shown). According to the obtained results, the established assay provides a fast, valuable, universally applicable and advantageous tool for substrate identification and allows limiting laborious turnover studies to investigate P450 BM3-catalyzed oxygenation *via* GC, HPLC, MS or NMR to those compounds that give positive results during this pre-screen. The general applicability is further supported by the low failure rate of inhibition screenings, which was reported to be below 0.8% (due to interference between

probe compounds and the formed fluorophores) by Fowler and Zhang based on a study of 5000 substances [90]. To the best of our knowledge, this is the first time coumarin-based substrates were used for inhibition studies with P450 BM3, which so far were limited to resorufin-based substrates. This progress was mainly enabled by the low K_M values obtained for the designed substrates (substrate **4**: 10.8 - 12.4 µM, substrate **5**: 3.1 - 3.4 µM), which are closer to those known for resorufin-substrates than for coumarin-derivatives and mirror the high native-substrate-resemblance of our compounds (e. g. 7-benzyloxyresorufin: 1.9 µM [39]; 7-ethoxyresorufin: 3.0 - 6.3 µM [41] and 7-allyloxyresorufin: 7.9 - 14.7 µM [42] vs. 7-ethoxycoumarin: 45 - 1220 µM [43] and BCCE: 25.2 - 34.3 µM [44]). On the contrary, the higher K_M values of thus far known coumarin-based substrates aggravated inhibition assays by necessitating high surrogate substrate amounts to assure sufficient activities. In addition, BCCE is only partly suited for inhibition assays as a hydrolysis step is required in addition to the P450 BM3-catalyzed hydroxylation to release the fluorophore and it is unknown which of these reactions is the rate-determining one.

Application to IC_{50} value determination

Despite of qualitative inhibition studies as shown in the preceding section, competitive inhibition assays also support quantitative screens for determination of IC_{50} values, which are measures for the affinity of compounds regarding the tested enzyme and can be considered as comparable with K_M or K_d values [59]. To prove the suitability of the established system for this purpose and to demonstrate the applicability of enzyme-substrate-pairs revealing low *O*-dealkylation activity for inhibition assays, the F87A mutant was used along with substrate **4** to determine the concentration-dependent inhibitory effect of benzoate **12**. Inhibition measurements were performed as described beforehand, except that the reaction time was exten-

ded and the concentration of substrate **4** was increased due to low enzyme activity (for kinetic parameters of F87A for substrate **4**, see Fig. S6 and Table S1 in the Supporting Information). Concentrations of benzoate **12** were set according to former studies and plotting against the respective inhibition values gave the hyperbolic curve shown in Fig. 4 [49]. Non-linear fitting revealed an IC_{50} value of 3.5 ± 0.4 µM, which correlates well with the previously determined K_M value of 3.7 ± 0.3 µM obtained in the conventional NADPH-consumption assay, thereby proving the established assay to be applicable for characterization of P450 BM3 mutants toward substrates and inhibitors [49].

Synthesis and characterization of a resorufin-derived analog

Resorufin-based screenings must be assumed as the main alternative regarding the established approach. Thus, the final step of the present study was the synthesis of a resorufin-derived analog of acid **4** to compare the synthetic useability of HTC **1** and resorufin (**18**) and their suitability as markers for generation of P450 BM3 substrates. As shown in Scheme 4 and according to the synthetic strategy described before, compound **7** was used for alkylation of phenol **18** giving the desired ester **19** in 61% yield. Noteworthy, higher solvent amounts and a longer reaction time were needed compared to the foregoing reaction due to low solubility of resorufin (**18**) and its derivatives. The subsequent saponification using KOH base failed due to decomposition of the starting material under alkaline conditions. Alternatively, the more pricy biocatalyst CalB enabled hydrolysis at almost neutral pH yielding acid **20** in 88%. The difficulties faced during this synthesis and the inferior overall yield of substrate **20** of 50% (compared to 88% achieved for the HTC-analog **4**) portend a lower suitability of resorufin (**18**) compared to HTC **1** for surrogate substrate synthesis from the chemical point of view and indicate that generation of more sophisticated substrates using

fluorophore **18** might be hampered. Moreover, decomposition of ether **19** was observed upon storage in solution (detectable by TLC) and hence, for the following experiments freshly prepared substrate samples were used. This instability of resorufin ethers has already been described by Klotz *et al.* in 1984; according to their studies 7-ethoxyresorufin stock solutions degraded to multiple UV-active products within 24 h [91]. Investigation of the optical properties of ethers **19** and **20** revealed that - in contrast to their HTC-analogs - these compounds are not fluorescent (optimal absorption wavelengths being λ_{abs}: 375 nm for **19** and λ_{abs}: 475 nm for **20**) and fluorophore **18** shows a smaller Stokes shift compared to **1** (Fig. 5). The solubility limits were determined to be 5.5 µM for ether **19** and 9.7 µM for ether **20** and hence, are 13 and 20 times lower compared to analogs **5** and **4**, respectively (see Fig. S4 in the Supporting Information). Activity measurements aiming at the detection of P450 BM3-mediated *O*-dealkylation of acid **20** failed due to degradation of this compound under assay conditions (proven *via* absorption of **20** at 475 nm, data not shown). Instability or P450 BM3-catalyzed oxygenation at the marker moiety were assumed as the most probable reasons for this observation, both rendering application of substrate **20** for *O*-dealkylation assays impossible. Hence, comparison of equally etherified HTC **1** and resorufin (**18**) was subsequently planned *via* the esters **5** and **19**. Pre-tests indicated that sufficient *O*-dealkylation of substrate **19** was solely mediated by the GQ double mutant, which showed the lowest activity for the HTC-labeled substrates beforehand, and respective kinetic analysis results are presented in Fig. 6. Interestingly, for this substrate no excess-substrate inhibition was observed, but - in contrast to **5** - the sigmoidal curve shape suggests positive homotropic cooperativity, which was confirmed by a Hill coefficient of $n = 2.1 \pm 0.1$ upon fitting of the obtained data. In addition, a K_M value of 1.8 ± 0.1 µM and a catalytic efficiency of

$0.458 \cdot 10^{-3}$ min^{-1} μM^{-1} were determined, the latter being 13 to 33 times lower compared to the values for ester **5**. The differences observed regarding the P450 BM3-mediated *O*-dealkylation of substrates **19** and **5** suggest different binding modes of these compounds within the enzyme, which might be of great interest for future protein engineering approaches. However, considering the obtained results, HTC **1** emerged as the better marker for the generation of fluorogenic P450 BM3 substrates as corresponding ethers showed higher stability, greater activity and better solubility compared to their resorufin analogs and provided a broader substrate spectrum for successful *O*-dealkylation screenings.

Conclusions

A novel, fluorescence-based and high-throughput-suited P450 BM3 assay was proven to be a promising, fast, easy, and reliable tool to carry out directed evolution of BM3 or identify potential substrates of this biocatalyst *via* inhibition studies. It is amenable to automation and adds a new feature to the existing panel of assays by accelerating screening efforts and increasing economic plus resource efficiency through substantial reagent conservation *via* high substrate yields and miniaturized formats. In detail, HTC **1** was proven to be a superior basis for the synthesis of P450 BM3 substrates compared to resorufin (**18**), since the corresponding ethers could be obtained in better yields and showed higher stability, activity and solubility plus wider applicability. The solubility aspect is especially interesting regarding multi-substrate applications (e. g. pooling of various substrates for enzyme fingerprints or assaying 'pseudo'-stereoisomers), which are further supported by the availability of coumarin derivatives with slightly different spectral properties. Moreover, the obtained results suggest that fluorophore **1** allows access to a broader substrate spectrum than fluorophore **18**. The designed, native-substrate-resembling, fluorogenic compounds

4 and **5** were fortunately hydroxylated by the tested P450 BM3 mutants under various conditions with high activities and led to the lowest K_M values observed to date for coumarin-based P450 BM3 substrates [43,44]. Thus, these substrates offer valuable tools for directed evolution campaigns targeting P450 BM3 features such as solvent resistance or (thermo)stability. In addition, according to Yun *et al.* the demand for highly active bacterial enzymes with human-like P450 activities will constantly grow to meet the needs of pharmaceutical research and bioremediation industries [25]. In this, P450 BM3 mutants are highly promising as they have been shown to fulfill these requirements and could repeatedly be engineered toward non-natural substrates. The established screening system allows studying P450 BM3 inhibition aiming at the identification of new substrates and hence, offers a new access to the desired mutants.

Acknowledgements

We thank the Ministry of Innovation, Science and Research of the German federal state of North-Rhine-Westphalia as well as the Heinrich Heine University Düsseldorf (scholarship within the CLIB-Graduate Cluster Industrial Biotechnology for K. N.) and are grateful to Shawn Whitfield for carefully revising the manuscript.

References

1 T. Omura, Forty years of cytochrome P450, Biochem. Biophys. Res. Commun. 266 (1999) 690-698.

2 E. M. J. Gillam, M. H. Hayes, The evolution of cytochrome P450 enzymes as biocatalysts in drug discovery and development, Curr. Top. Med. Chem. 13 (2013) 2254-2280.

3 V. B. Urlacher, M. Girhard, Cytochrome P450 monooxygenases: an update on perspectives for synthetic application, Trends Biotechnol. 30 (2012) 26-36.

4 R. Fasan, Tuning P450 enzymes as oxidation catalysts, ACS Catal. 2 (2012) 647-666.

5 S. Kumar, Engineering cytochrome P450 biocatalysts for biotechnology, medicine and bioremediation, Expert Opin. Drug Metab. Toxicol. 6 (2010) 115-131.

6 R. Bernhardt, Cytochromes P450 as versatile biocatalysts, J. Biotechnol. 124 (2006) 128-145.

7 E. Roduner, W. Kaim, B. Sarkar, V. B. Urlacher, J. Pleiss, R. Gläser, W.-D. Einicke, G. A. Sprenger, U. Beifuß, E. Klemm, C. Liebner, H. Hieronymus, S.-F. Hsu, B. Plietker, S. Laschat, Selective catalytic oxidation of C-H bonds with molecular oxygen, ChemCatChem 54 (2013) 82-112.

8 C. J. C. Whitehouse, S. G. Bell, L.-L. Wong, $P450_{BM3}$ (CYP102A1): connecting the dots, Chem. Soc. Rev. 41 (2012) 1218-1260.

9 S. Pflug, S. M. Richter, V. B. Urlacher, Development of a fed-batch process for the production of the cytochrome P450 monooxygenase CYP102A1 from *Bacillus megaterium* in E. coli, J. Biotechnol. 129 (2007) 481-488.

10 U. Schwaneberg, A. Sprauer, C. Schmidt-Dannert, R. D. Schmid, P450 monooxygenase in biotechnology I. Single-step, large-scale purification method for cytochrome P450 BM-3 by anion-exchange chromatography. J. Chromatogr. A 848 (1999) 149-159.

11 A. W. Munro, D. G. Ley, K. J. McLean, K. R. Marshall, T. W. B. Ost, S. Daff, C. S. Miles, S. K. Chapman, D. A. Lysek, C. C. Moder, C. C. Page, P. L. Dutton, P450 BM3: the very model of a modern flavocytochrome, Trends Biochem. Sci. 27 (2002) 250-257.

12 S. T. Jung, R. Lauchli, F. H. Arnold, Cytochrome P450: taming a wild type enzyme, Curr. Opin. Biotechnol. 22 (2011) 809-817.

13 J. C. Lewis, F. H. Arnold, Catalysts on demand: selective oxidations by laboratory-evolved cytochrome P450 BM3, Chimia 63 (2009) 309-312.

14 R. Agudo, G.-D. Roiban, M. T. Reetz, Achieving regio- and enantioselectivity of P450-catalyzed oxidative CH activation of small functionalized molecules by structure-guided directed evolution, ChemBioChem 13 (2012) 1465-1473.

15 A. Rentmeister, F. H. Arnold, R. Fasan, Chemo-enzymatic fluorination of unactivated organic compounds, Nat. Chem. Biol. 5 (2009) 26-28.

16 K. Kühnel, S. C. Maurer, Y. Galeyeva, W. Frey, S. Laschat, V. B. Urlacher, Hydroxylation of dodecanoic acid and (2R, 4R,6R,8R)-tetramethyldecanol on a

preparative scale using an NADPH-dependent CYP102A1 mutant, Adv. Synth. Catal. 349 (2007) 1451-1461.

17 S. C. Maurer, K. Kühnel, L. A. Kaysser, S. Eiben, R. D. Schmid, V. B. Urlacher, Catalytic hydroxylation in biphasic systems using CYP102A1 mutants, Adv. Synth. Catal. 347 (2005) 1090-1098.

18 D. F. Münzer, P. Meinhold, M. W. Peters, S. Feichtenhofer, H. Griengl, F. H. Arnold, A. Glieder, A. de Raadt, Stereoselective hydroxylation of an achiral cyclopentanecarboxylic acid derivative using engineered P450s BM-3, Chem. Commun. (2005) 2597-2599.

19 S. Schneider, M. G. Wubbolts, G. Oesterhelt, D. Danglard, B. Witholt, Controlled regioselectivity of fatty acid oxidation by whole cells producing cytochrome $P450_{BM-3}$ monooxygenase under varied dissolved oxygen concentrations, Biotechnol. Bioeng. 64 (1999) 333-341.

20 L.-L. Wong, $P450_{BM3}$ on steroids: the swiss army knife P450 enzyme just gets better, ChemBioChem 12 (2011) 2537-2539.

21 J. A. Dietrich, Y. Yoshikuni, K. J. Fisher, F. X. Woolard, D. Ockey, D. J. McPhee, N. S. Renninger, M. C. Y. Chang, D. Baker, J. D. Deasling, A novel semi-biosynthetic route for artemisinin production using engineered substrate-promiscuous $P450_{BM3}$, ACS Chem. Biol. 4 (2009) 261-267.

22 V. Rea, D. Falck, J. Kool, F. J. J. de Kanter, J. N. M. Commandeur, N. P. E. Vermeulen, W. M. A. Niessen, M. Honing, Combination of biotransformation by P450 BM3 mutants with on-line post-column bioaffinity and mass spectrometric

profiling as a novel strategy to diversify and characterize p38α kinase inhibitors, Med. Chem. Commun. 4 (2013) 371-377.

23 G. Di Nardo, G. Gilardi, Optimization of the bacterial cytochrome P450 BM3 system for the production of human drug metabolites, Int. J. Mol. Sci. 13 (2012) 13, 15901-15924.

24 T. A. Baillie, Metabolism and toxicity of drugs. Two decades of progress in industrial drug metabolism, Chem. Res. Toxicol. 21 (2008) 129-137.

25 J. M. Caswell, M. O'Neill, S. J. C. Taylor, T. S. Moody, Engineering and application of P450 monooxygenases in pharmaceutical and metabolite synthesis, Curr. Opin. Chem. Biol. 17 (2013) 271-275.

26 C.-H. Yun, K.-H. Kim, D.-H. Kim, H.-C. Jung, J.-G. Pan, The bacterial P450 BM3: a prototype for a biocatalyst with human P450 activities, Trends Biotechnol. 25 (2007) 289-298.

27 V. B. Urlacher, S. Lutz-Wahl, R. D. Schmid, Microbial P450 enzymes in biotechnology, Appl. Microbiol. Biotechnol. 64 (2004) 317-325.

28 V. B. Urlacher, R. D. Schmid, Biotransformations using prokaryotic P450 monooxygenases, Curr. Opin. Biotechnol. 13 (2002) 557-564.

29 K. L. Tee, U. Schwaneberg, Directed evolution of oxygenases: screening systems, success stories and challenges, Comb. Chem. High Throughput Screening 10 (2007) 197-217.

30 U. Schwaneberg, C. Schmidt-Dannert, J. Schmitt, R. D. Schmid, A continuous spectrophotometric assay for P450 BM-3, a fatty acid hydroxylating enzyme, and its mutant F87A, Anal. Biochem. 269 (1999) 359-366.

31 J.-L. Reymond, Substrate arrays for fluorescence-based enzyme fingerprinting and high-throughput screening, Ann. N. Y. Acad. Sci. 1130 (2008) 12-20.

32 E. O'Reilly, V. Köhler, S. L. Flitsch, N. J. Turner, Cytochromes P450 as useful biocatalysts: addressing the limitations. Chem. Commun. 47 (2011) 2490-2501.

33 G. F. da Cruz, C. F. F. Angolini, L. G. de Oliveira, P. F. Lopes, S. P. de Vasconcellos, E. Crespim, V. M. de Oliveira, E. V. dos Santos Neto, A. J. Marsaioli, Searching for monooxygenases and hydrolases in bacteria from an extreme environment, Appl. Microbiol. Biotechnol. 87 (2010) 319-329.

34 R. Zhang, K.-D. Kang, G. Shan, B. D. Hammock, Design, synthesis and evaluation of novel P450 fluorescent probes bearing α-cyanoether, Tetrahedron Lett. 44 (2003) 4331-4334.

35 J. L. Wahlstrom, D. A. Rock, J. G. Slatter, L. C. Wienkers, Advances in predicting CYP-mediated drug interactions in the drug discovery setting, Expert Opin. Drug Discovery 1 (2006) 677-691.

36 G. Zlokarnik, P. D. J. Grootenhuis, J. B. Watson, High throughput P450 inhibition screens in early drug discovery, Drug Discovery Today 10 (2005) 1443-1450.

37 L. C. Wienkers, T. G. Heath, Predicting *in vivo* drug inteactions from in vitro drug discovery data, Nat. Rev. 4 (2005) 825-833.

38 C. L. Crespi, V. P. Miller, B. W. Penman, Microtiter plate assays for inhibition of human, drug-metabolizing cytochrome P450, Anal. Biochem. 248 (1997) 188-190.

39 B. M. A. Lussenburg, L. C. Babel, N. P. E. Vermeulen, J. N. M. Commandeur, Evaluation of alkoxyresorufins as fluorescent substrates for cytochrome P450 BM3 and site-directed mutants, Anal. Biochem. 341 (2005) 148-155.

40 E. Vottero, V. Rea, J. Lastdrager, M. Honing, N. C. E. Vermeulen, J. N. M. Commandeur, Role of residue 87 in substrate selectivity and regioselectivity of drug-metabolizing cytochrome P450 CYP102A1 M11, J. Biol. Inorg. Chem. 16 (2011) 899-912.

41 D.-H. Kim, K.-H. Kim, D. Kim, H.-C. Jung, J.-G. Pan, Y.-T. Chi, T. Ahn, C.-H. Yun, Oxidation of human cytochrome P450 1A2 substrates by *Bacillus megaterium* cytochrome P450 BM3, J. Mol. Catal. B: Enzym. 63 (2010) 179-187.

42 J. Reinen, S. Ferman, E. Vottero, N. P. E. Vermeulen, J. N. M. Commandeur, Application of a fluorescence-based continuous-flow bioassay to screen for diversity of cytochrome P450 BM3 mutant libraries, J. Biomol. Screening 16 (2011) 239-250.

43 D.-H. Kim, K.-H. Kim, D.-H. Kim, K.-H. Liu, H.-C. Jung, J.-G. Pan, C.-H. Yun, Generation of human metabolites of 7-ethoxycoumarin by bacterial cytochrome P450 BM3, Drug Metab. Dispos. 36 (2008) 2166-2170.

44 A. J. Ruff, A. Dennig, G. Wirtz, M. Blanusa, U. Schwaneberg, Flow cytometer-based high-throughput screening system for accelerated directed evolution of P450 monooxygenases, ACS Catal. 2 (2012) 2724-2728.

45 M. A. Noble, C. S. Miles, S. K. Chapman, D. A. Lysek, A. C. Mackay, G. A. Reid, R. P. Janzlik, A. W. Munro, Roles of key active-site residues in flavocytochrome P450 BM3, Biochem. J. 339 (1999) 371-379.

46 V. E. V. Ferrero, G. Di Nardo, G. Catucci, S. J. Sadeghi, G. Gilardi, Fluorescence detection of ligand binding to labeled cytochrome P450 BM3, Dalton Trans. 41 (2012) 2018-2025.

47 A. Verras, I. D. Kuntz, P. R. Ortiz de Montellano, in: D. C. Spellmeyer (Ed.), Annual Reports in Computational Chemisty, Vol. 2, Elsevier, 2006, pp. 171-195.

48 C. Oostenbrink, A. de Ruiter, J. Hritz, N. Vermeulen, Malleability and versatility of cytochrome P450 active sites studied by molecular simulations, Curr. Drug. Metab. 13 (2012) 190-196.

49 K. Neufeld, J. Marienhagen, U. Schwaneberg, J. Pietruszka, Benzylic hydroxylation of aromatic compounds by P450 BM3, Green Chem. 15 (2013) 2408-2421.

50 M. Katkevičs, A. Kontijevskis, I. Mutule, E. Sũna, Microwave-promoted automated synthesis of a coumarin library, Chem. Heterocycl. Compd. 43 (2007) 151-159.

51 H. Wang, Magnesium bis(trifluoromethane)sulfonimide: an efficient catalyst for the synthesis of coumarins under solvent-free conditions, Monats. Chem. 144 (2013) 411-414.

52 H. Shabany, R. Pajewski, E. Abel, A. Mukhopadhyay, G. W. Gokel, The effect of twin-tailed sidearms on sodium cation transport in synthetic hydraphile cation channels, J. Heterocycl. Chem. 38 (2001) 1393-1400.

53 Drug Delivery System Institute, Ltd.; EP953357 A1, 1999.

54 Quonova LLC; WO2009/77844 A2, 2009.

55 G. H: Jones, M. C. Venuti, R. Alvarez, J. J. Bruno, A. H. Berks, A. Prince, Inhibitors of cyclic AMP phosphodiesterase. 1. Analogues of cilostamide and anagrelide, J. Med. Chem. 30 (1987) 295-303.

56 Hill equation was modified according to equation 5.44 in: R. A. Copeland, Enzymes: a practical introduction to structure, mechanism, and data analysis, 2nd edition, Wiley, 2000.

57 M. T. Donato, N. Jiménez, J. V. Castell, M. J. Gómez-Lechón, Fluorescence-based assays for screening nine cytochrome P450 (P450) activities in intact cells expressing individual human P450 enzymes, Drug. Metab. Dispos. 32 (2004) 699-706.

58 J.-P. Goddard, J.-L. Reymond, Recent advances in enzyme assays, Trends Biotechnol. 22 (2004) 363-370.

59 B. D. Marks, R. W. Smith, H. A. Braun, T. A. Goossens, M. Christenson, M. S. Ozers, C. S. Lebakken, O. V. Trubetskoy, A high throughput screening assay to screen for CYP2E1 metabolism and inhibition using a fluorogenic Vivid® P450 substrate, Assay Drug Dev. Technol. 1 (2002) 73-81.

60 L. O. Narhi, A. J. Fulco, Characterisation of a catalytically self-sufficient 119,000-Dalton cytochrome P-450 monooxygenase induced by barbiturates in *Bacillus megaterium*, J. Biol. Chem. 261 (1986) 7160-7169.

61 N. Kawakami, O. Shoji, Y. Watanabe, Direct hydroxylation of primary carbons in small alkanes by wild-type cytochrome P450BM3 containing perfluorocarboxylic acids as decoy molecules, Chem. Sci. 4 (2013) 2344-2348.

62 F. E. Zilly, J. P. Acevedo, W. Augustyniak, A. Deege, U. W. Häusig, M. T. Reetz, Tuning a P450 enzyme for methane oxidation, Angew. Chem. 123 (2011) 2772-2776.

63 N. Kawakami, O. Shoji, Y. Watanabe, Use of perfluorocarboxylic acids to trick cytochrome P450BM3 into initiating the hydroxylation of gaseous alkanes, Angew. Chem. Int. Ed. 50 (2011) 5315-5318.

64 H. Amii, K. Uneyama, C-F bond activation in organic synthesis, Chem. Rev. 109 (2009) 2119-2183.

65 E. Kitamura, T. Otomatsu, C. Maeda, Y. Aoki, C. Ota, N. Misawa, K. Shindo, Production of hydroxylated flavonoids with cytochrome P450 BM3 variant F87V and their antioxidative activities, Biosci., Biotechnol., Biochem. 77 (2013) 1340-1343.

66 S. Staudt, C. A. Müller, J. Marienhagen, C. Böing, S. Buchholz, U. Schwaneberg, H. Gröger, Biocatalytic hydroxylation of *n*-butane with *in situ* cofactor regeneration at low temperature and under normal pressure, Beilstein J. Org. Chem. 8 (2012) 186-191.

67 D. Zehentgruber, V. B. Urlacher, S. Lütz, Studies on the enantioselective oxidation of β-ionone with a whole *E. coli* system expressing cytochrome P450 monooxygenase BM3, J. Mol. Catal. B: Enzym. 84 (2012) 62-64.

68 N. Misawa, M. Nodate, T. Otomatsu, K. Shimizu, C. Kaido, M. Kikuta, A. Ideno, H. Ikenaga, J. Ogawa, S. Shimizu, K. Shindo, Bioconversion of substituted naphthalenes and β-eudesmol with the cytochrome P450 BM3 variant F87V, Appl. Microbiol. Biotechnol. 90 (2011) 147-157.

69 R. J. F. Branco, A. Seifert, M. Budde, V. B. Urlacher, M. J. Ramos, J. Pleiss, Anchoring effects in a wide binding pocket: the molecular basis of regioselectivity in engineering cytochrome P450 monooxygenase from *B. megaterium*, Proteins 73 (2008) 597-607.

70 Y. Watanabe, S. Laschat, M. Budde, O. Affolter, Y. Shimada, V. B. Urlacher, Oxidation of acyclic monoterpenes by P450 BM-3 monooxygenase: influence of the substrate *E*/*Z*-isomerism on enzyme chemo- and regioselectivity, Tetrahedron 63 (2007) 9413-9422.

71 W. T. Sulistyaningdyah, J. Ogawa, Q.-S. Li, C. Maeda, Y. Yano, R. D. Schmid, S. Shimizu, Hydroxylation activity of P450 BM-3 mutant F87V towards aromatic compounds and its application to the synthesis of hydroquinone derivatives from phenolic compounds, Appl. Microbiol. Biotechnol. 67 (2005) 556-562.

72 D. Appel, S. Lutz-Wahl, P. Fischer, U. Schwaneberg, R. D. Schmid, A P450 BM-3 mutant hydroxylates alkanes, cycloalkanes, arenes and heteroarenes, J. Biotechnol. 88 (2001) 167-171.

73 Q.-S. Li, J. Ogawa, R. D. Schmid, S. Shimizu, Engineering cytochrome P450 BM-3 for oxidation of polycyclic aromatic hydrocarbons, Appl. Environ. Microbiol. 67 (2001) 5735-5739.

74 S. Graham-Lorence, G. Truan, J. A. Peterson, J. R. Falck, S. Wei, C. Helvig, J. H. Capdevila, An active site substitution, F87V, converts cytochrome P450 BM-3 into a regio- and stereoselective (14S,15R)-arachidonic acid epoxygenase, J. Biol. Chem. 272 (1997) 1127-1135.

75 J. Kuper, K. L. Tee, M. Wilmanns, D. Roccatano, U. Schwaneberg, T. S. Wong, The role of active-site Phe87 in modulating the organic co-solvent tolerance of cytochrome P450 BM3 monooxygenase, Acta Crystallogr., Sect. F: Struct. Biol. Cryst. Commun. 68 (2012) 1013-1017.

76 Q.-S. Li, J. Ogawa, R. D. Schmid, S. Shimizu, Residue size at position 87 of cytochrome P450 BM-3 determines its stereoselectivity in propylbenzene and 3-chlorostyrene oxidation, FEBS Lett. 508 (2001) 249-252.

77 C. F. Oliver, S. Modi, M. J. Sutcliffe, W. U. Primrose, L.-Y. Lian, G. C. K. Roberts, A single mutation in cytochrome P450 BM3 changes substrate orientation in a catalytic intermediate and the regiospecificity of hydroxylation, Biochemistry 36 (1997) 1567-1572.

78 J. Reymond, Modern Biocatalysis: stereoselective and environmentally friendly reactions, Wiley, 2009.

79 D. E. T. Pazmiño, M. Winkler, A. Glieder, M. W. Fraaije, Monooxygenases as biocatalysts: classification, mechanistic aspects and biotechnological applications, J. Biotechnol. 146 (2010) 9-24.

80 T. S. Wong, F. H. Arnold, U. Schwaneberg, Laboratory evolution of cytochrome P450 BM-3 monooxygenase for organic cosolvents, Biotechnol. Bioeng. 85 (2004) 351-358.

81 H. Tsubery, I. Ofek, S. Cohen, M. Fridkin, Structure-function studies of polymyxin B nonapeptide: implications to sensitization of gram-negative bacteria, J. Med. Chem. 43 (2000) 3085-3092.

82 U. Schwaneberg, C. Otey, P. C. Cirino, E. Farinas, F. H. Arnold, Cost-effective whole-cell assay for laboratory evolution of hydroxylases in *Escherichia coli*, J. Biomol. Screening 6 (2001) 111-117.

83 W. M. Atkins, Non-Michaelis-Menten kinetics in cytochrome P450-catalyzed reactions, Annu. Rev. Pharmacol. Toxicol. 45 (2005) 291-310.

84 Y. Lin, P. Lu, C. Tang, Substrate inhibition kinetics for cytochrome P450-catalyzed reactions, Drug Metab. Dispos. 29 (2001) 368-374.

85 R. Neeli, H. M. Girvan, A. Lawrence, M. J. Warren, D. Leys, N. S. Scrutton, A. W. Munro, The dimeric form of flavocytochrome P450 BM3 is catalytically functional as a fatty acid hydroxylase, FEBS Lett. 579 (2005) 5582-5588.

86 S. S. Boddupalli, B. C. Pramanik, C. A. Slaughter, R. W. Estabrook, J. A. Peterson, Fatty acid monooxygenation by $P450_{BM-3}$: product identification and proposed mechanism for the sequential hydroxylation reactions, Arch. Biochem. Biophys. 292 (1992) 20-28.

87 S. J. Smith, A. W. Munro, W. E. Smith, Resonance raman scattering of cytochrome P450 BM3 and effect of imidazole inhibitors, Biopolymers 70 (2003) 620-627.

88 T. W. B. Ost, J. P. Clark, J. L. R. Anderson, L. J. Yellowlees, S. Daff, S. K. Chapman, 4-Cyanopyridine, a versatile spectroscopic probe for cytochrome P450 BM3, J. Biol. Chem. 279 (2004) 48876-48882.

89 G. Di Nardo, A. Fantuzzi, A. Sideri, P. Panicco, C. Sassone, C. Giunta, G. Gilardi, Wild-type CYP102A1 as a biocatalyst: turnover of drugs usually metabolized by human liver enzymes, J. Biol. Inorg. Chem. 12 (2007) 313-323.

90 S. Fowler, H. Zhang, *In vitro* evaluation of reversible and irreversible cytochrome P450 inhibition: current status on methodologies and their utility for predicting drug-drug interactions, AAPS J. 10 (2008) 410-424.

91 A. V. Klotz, J. J. Stegeman, C. Walsh, An alternative 7-ethoxyresorufin O-deethylase activity assay: a continuous visible spectrophotometric method for measurement of cytochrome P-450 monooxygenase activity, Anal. Biochem. 140 (1984) 138-145.

Footnotes

[1] The project "ExpresSys" was funded by the BMBF in the framework of the funding measure GenoMik (http://genomik-transfer.de/en/index_en.php?section=home).

[2] *Abbreviations used*: ADH_{LK}, alcohol dehydrogenase from *Lactobacillus kefir*; AGE, agarose gel electrophoresis; BCCE, 7-benzyloxy-3-carboxycoumarin ethyl ester; BM3 buffer, KPi/Tris-buffer-mixture (50 mM KPi, 50 mM Tris/HCl, pH 7.8); CalB, lipase B from *Candida antarctica*; CCL, cell-free crude lysate; f. c., final concentration; FDH, formate dehydrogenase; GDH, glucose dehydrogenase; GQ, P450 BM3 mutant A74G L188Q; GV, P450 BM3 mutant A74G F87V; GVQ, P450 BM3 mutant A74G F87V L188Q; HTC, 7-hydroxy-4-(trifluoromethyl)coumarin; IC_{50}: inhibitor concentration required to reduce enzyme activity by 50%; K_i, substrate concentration at which enzyme activity is reduced by 50% ($K_M < K_i$); λ_{abs}, absorption maximum; λ_{ex}, excitation maximum; λ_{em}, emission maximum; n, Hill coefficient; MW, microwave; P450, cytochrome P450 monooxygenase; PE, petroleum ether; VQ, P450 BM3 mutant F87V L188Q.

Tables

Table 1: Rates of *O*-dealkylation of substrate **4** by P450 BM3 mutants using different NADPH-recycling-systems compared to the NADPH-based approach (e.v.: empty vector).

P450 BM3 mutant	NADPH	GDH-recycling	FDH-recycling	ADH-recycling
highest activity values of measurement series in pmol/5min:				
GV	58.2 ± 4.3	70.3 ± 4.6	44.9 ± 2.6	101.4 ± 4.1
reaction rates relative to the highest activity values in %:				
A74G	19 ± 3	12 ± 2	18 ± 5	13 ± 1
F87V	55 ± 11	50 ± 7	70 ± 1	36 ± 2
L188Q	29 ± 9	12 ± 5	21 ± 6	12 ± 1
GV	100 ± 7	100 ± 7	100 ± 6	100 ± 4
GQ	19 ± 2	14 ± 1	20 ± 7	15 ± 3
VQ	45 ± 4	39 ± 2	60 ± 12	32 ± 2
GVQ	42 ± 11	23 ± 4	36 ± 2	22 ± 3
F87A	15 ± 5	13 ± 2	19 ± 3	10 ± 2
WT	12 ± 5	8 ± 2	16 ± 2	10 ± 1
e.v.	0 ± 6	0 ± 1	0 ± 4	0 ± 0

Table 2: Rates of *O*-dealkylation of substrate **4** by P450 BM3 mutants using different biocatalyst sources compared to the cell-free crude lysate approach (e.v.: empty vector).

P450 BM3 variant	cell-free crude lysates	untreated whole-cells	polymyxin B-permeabilized cells	lysozyme-lysed cells
highest activity values of measurement series in pmol/5min:				
GV	70.3 ± 4.6	11.9 ± 1.1	9.8 ± 1.2	50.0 ± 6.1
reaction rates relative to the highest activity values in %:				
A74G	12 ± 2	37 ± 5	57 ± 1	21 ± 3
F87V	50 ± 7	69 ± 9	66 ± 4	64 ± 20
L188Q	12 ± 5	1 ± 3	10 ± 5	7 ± 0
GV	100 ± 7	100 ± 9	100 ± 12	100 ± 12
GQ	14 ± 1	28 ± 6	50 ± 5	21 ± 7
VQ	39 ± 2	69 ± 14	64 ± 18	47 ± 16
GVQ	23 ± 4	52 ± 14	61 ± 14	34 ± 2
F87A	13 ± 2	22 ± 5	29 ± 9	19 ± 3
WT	8 ± 2	37 ± 9	44 ± 7	22 ± 2
e.v.	0 ± 1	0 ± 4	0 ± 4	0 ± 4

Table 3: Kinetic parameters of P450 BM3-mediated *O*-dealkylation of fluorogenic substrates **4** and **5**. Data were fitted to a modified Hill equation considering excess-substrate inhibition.[30]

kinetic parameters	substrate 4			substrate 5	
	A74G/F87V	F87V	A74G/L188Q	A74G/F87V	F87V
k_{cat} [min^{-1}]	5.683 ± 1.061	2.242 ± 0.353	0.123 ± 0.019	0.020 ± 0.008	0.045 ± 0.008
K_M [µM]	12.4 ± 2.5	10.8 ± 2.4	12.3 ± 2.0	3.4 ± 1.9	3.1 ± 1.0
k_{cat}/K_M [min^{-1} μM^{-1}]	0.458	0.208	0.010	0.006	0.015
K_i [µM]	200.0 ± 64.1	253.4 ± 84.6	254.0 ± 76.1	57.8 ± 38.9	51.7 ± 13.9
n	2.2 ± 0.5	1.7 ± 0.4	2.1 ± 0.3	1.4 ± 0.4	1.4 ± 0.2
chi^2	1.670	0.665	1.507	3.357	2.221
R^2	0.985	0.989	0.982	0.961	0.994

Table 4: Inhibition of P450 BM3-mediated *O*-dealkylation of substrate **4** by known substrates, non-substrates and inhibitors.

probe compound	compound concentration	P450 BM3 activity [%][a]	
		A74G/F87V	F87V
DMSO	---	100 ± 1	100 ± 1
myristic acid (**10**)	200 µM	47 ± 3	48 ± 1
	100 µM	66 ± 5	61 ± 2
	20 µM	-	87 ± 1
naphthalene (**11**)	5 mM	39 ± 0	40 ± 2
	1 mM	66 ± 5	44 ± 4
	100 µM	-	82 ± 2
methyl 2-methoxy-3-methylbenzoate (**12**)	5 mM	48 ± 5	56 ± 3
	1 mM	88 ± 2	-
	100 µM	-	-
ketoconazole (**13**)	5 µM	13 ± 1	9 ± 1
	1µmM	65 ± 4	83 ± 4
	200 nM	-	-
imidazole (**14**)	5 mM	2 ± 1	22 ± 1
	1 mM	80 ± 1	-
	100 µM	-	-
potassium cyanide (**15**)	5 mM	61 ± 3	39 ± 1
	1 mM	73 ± 5	49 ± 5
	100 µM	87 ± 0	-
	20 µM	-	-
caffeine (**16**)	5 mM	-	-
	1 mM	-	-
	100 µM	-	-
isooctane (**17**)	5 mM	-	-
	1 mM	-	-
	100 µM	-	-

[a] Activities are reported relative to the DMSO-reference sample in absence of a probe compound and a threshold value of 90%.

Scheme Legends

Scheme 1: Synthesis of fluorophore **1** (MW: microwave).

Scheme 2: Synthesis of surrogate substrate **4**.

Scheme 3: Principle of the fluorogenic assay using the example of substrate **4**.

Scheme 4: Synthesis of surrogate substrate **20**.

Figure Legends

Figure 1: Normalized absorption (solid, black lines), excitation (solid, grey lines) and emission spectra (dashed lines) of fluorophore **1**, acid **4** and ester **5**; 10 µM compound in BM3 buffer with 10 vol% DMSO.

Figure 2: Rates of *O*-dealkylation of substrate **4** by P450 BM3 mutants in the presence of NADPH (e.v.: empty vector).

Figure 3: Enzyme activity as a function of substrate concentration for P450 BM3 mutant A74G/F87V with substrate **4** (left) and F87V with substrate **5** (right) displaying excess-substrate inhibition.

Figure 4: Inhibitory effect of substrate **12** on F87A-mediated *O*-dealkylation of **4**. Data were fitted to Michaelis-Menten equation (chi^2: 5.779, R^2: 0.990).

Figure 5: Normalized absorption (solid, black lines), excitation (solid, grey line) and emission spectra (dashed line) of resorufin (**18**), ester **19** and acid **20**; 10 µM compound in BM3 buffer with 10 vol% DMSO.

Figure 6: Michaelis-Menten plot for P450 BM3 mutant A74G/L188Q with substrate **19**. Data were fitted to Hill equation (chi^2: 0.520, R^2: 0.997).

Fig. 1.

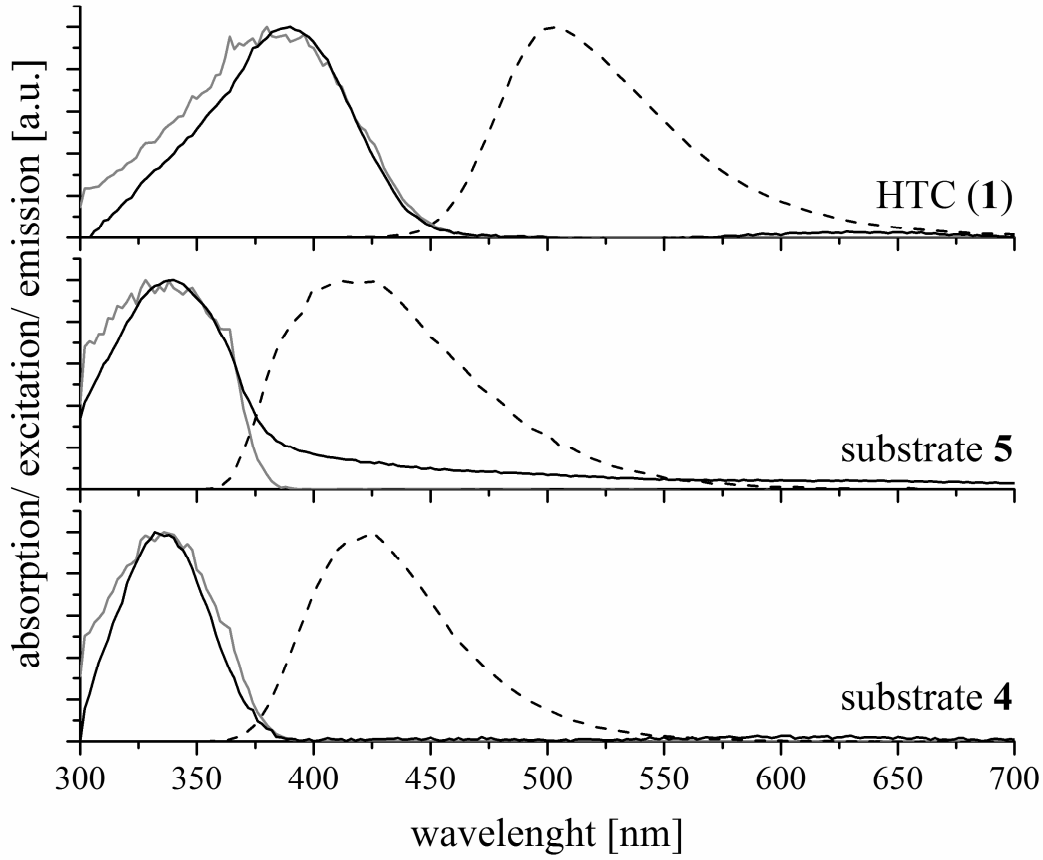

Fig. 2.

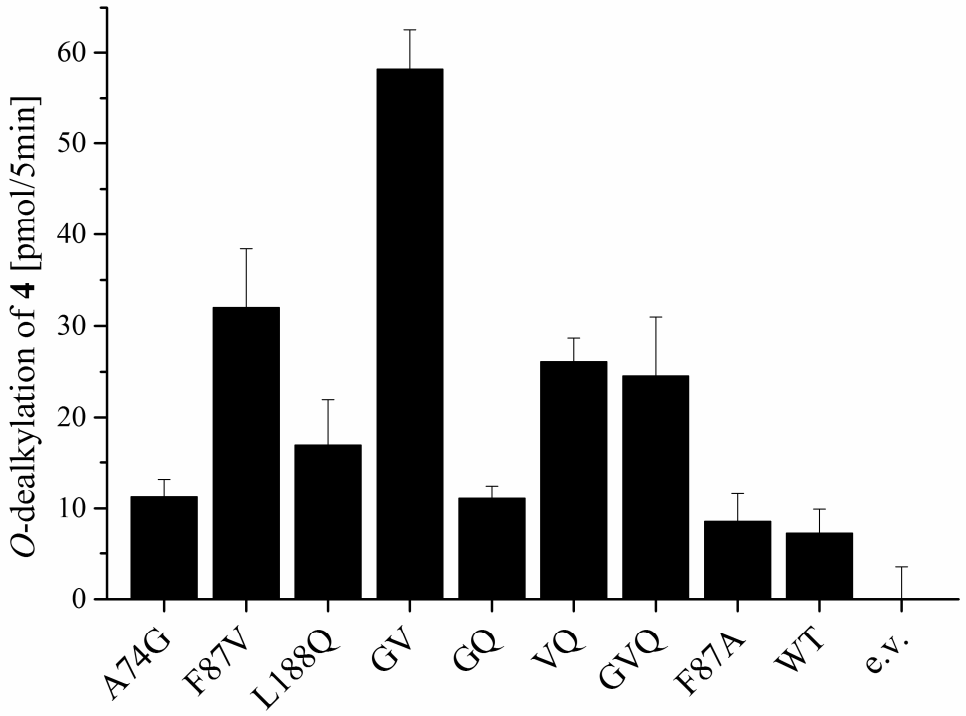

Fig. 3.

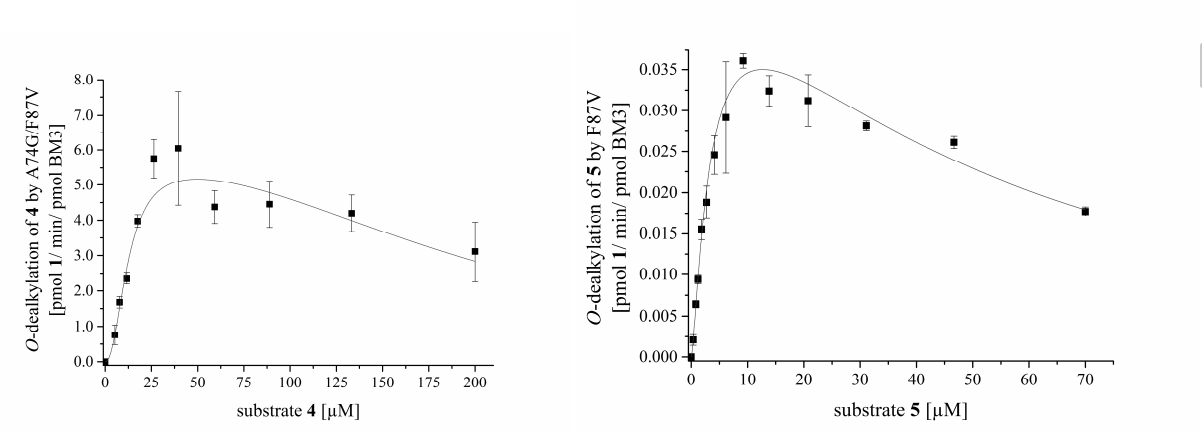

Fig. 4.

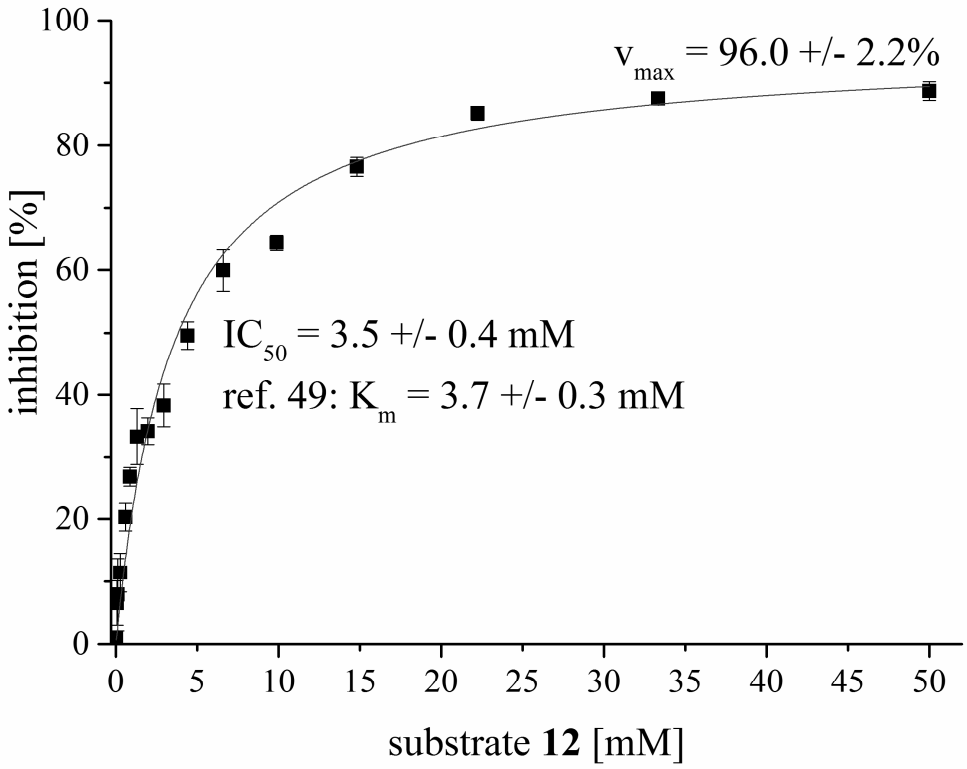

Fig. 5.

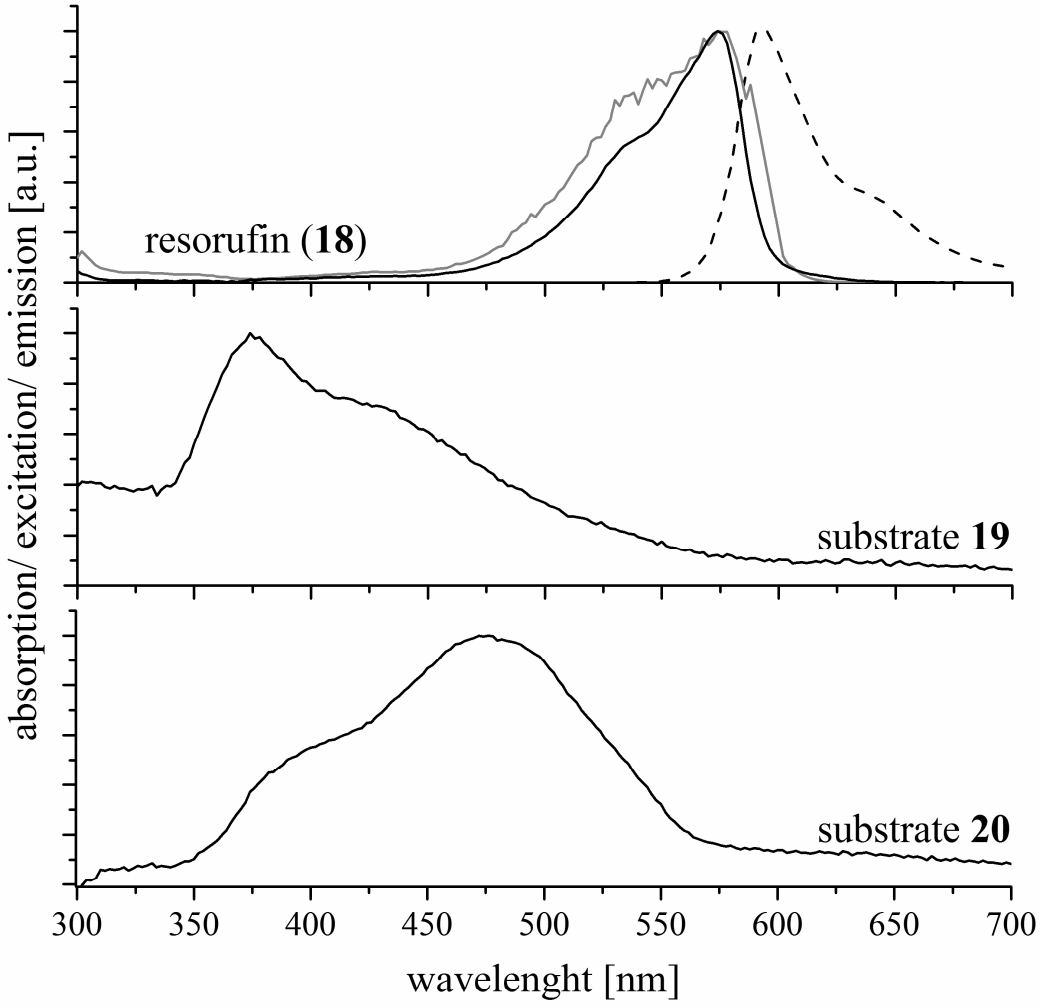

Fig. 6.

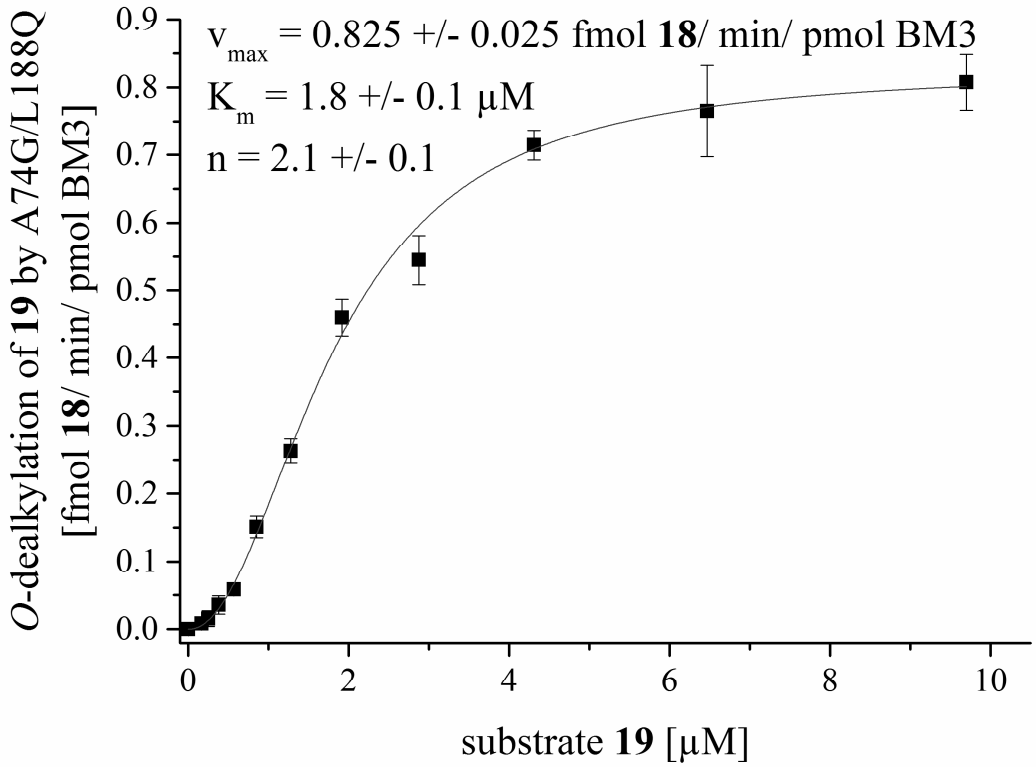

Scheme 1.

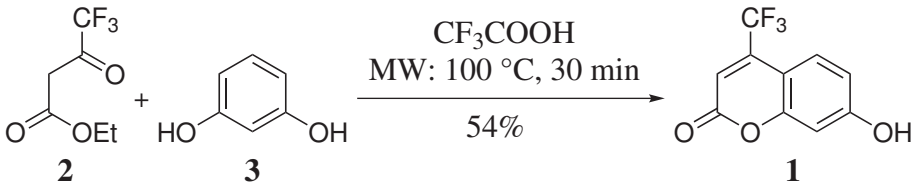

Scheme 2.

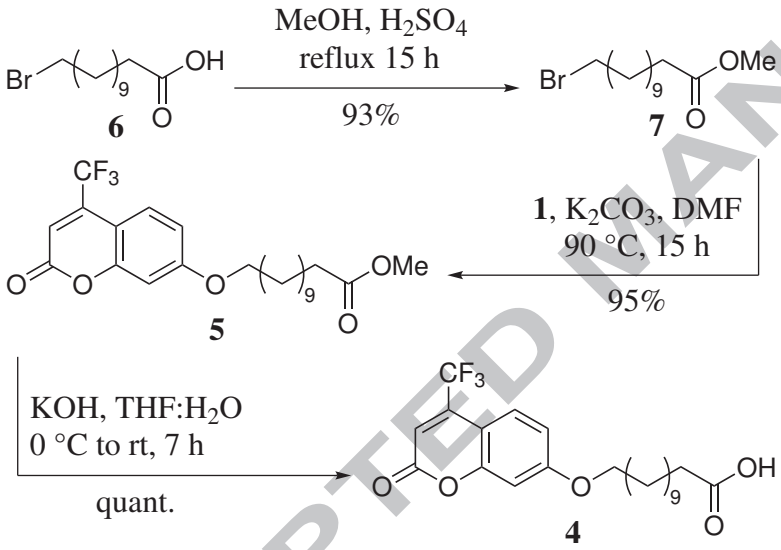

Scheme 3

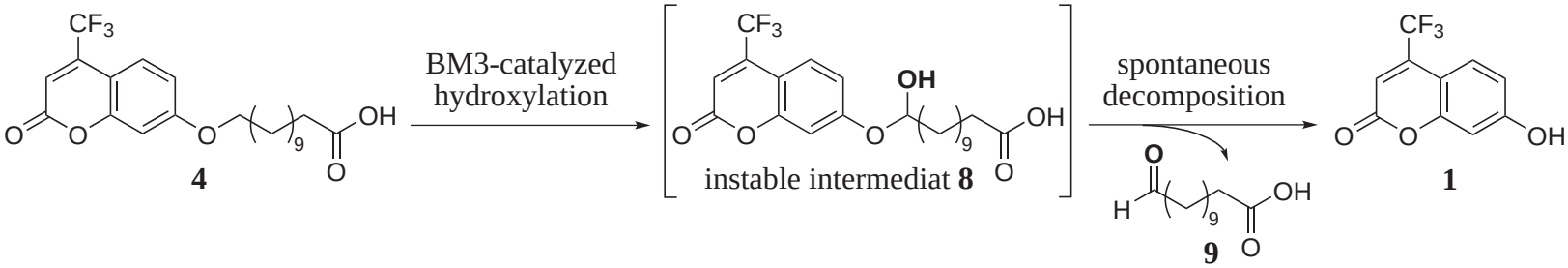

Scheme 4

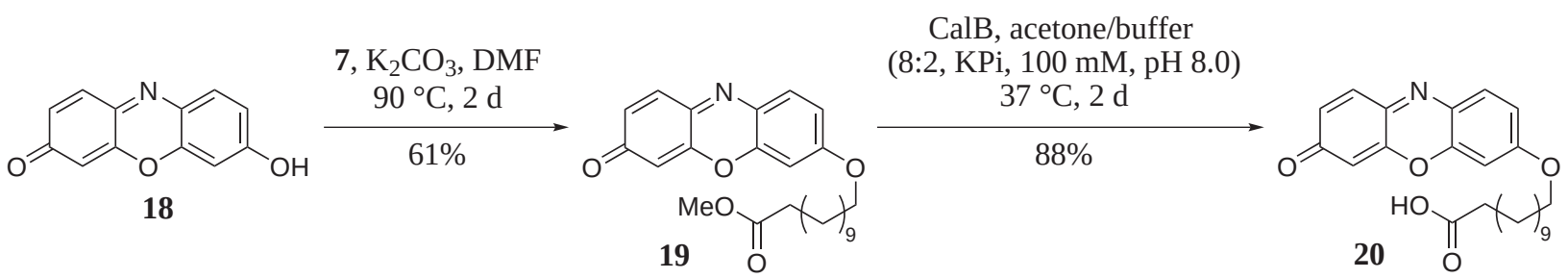

18 **19** **20**